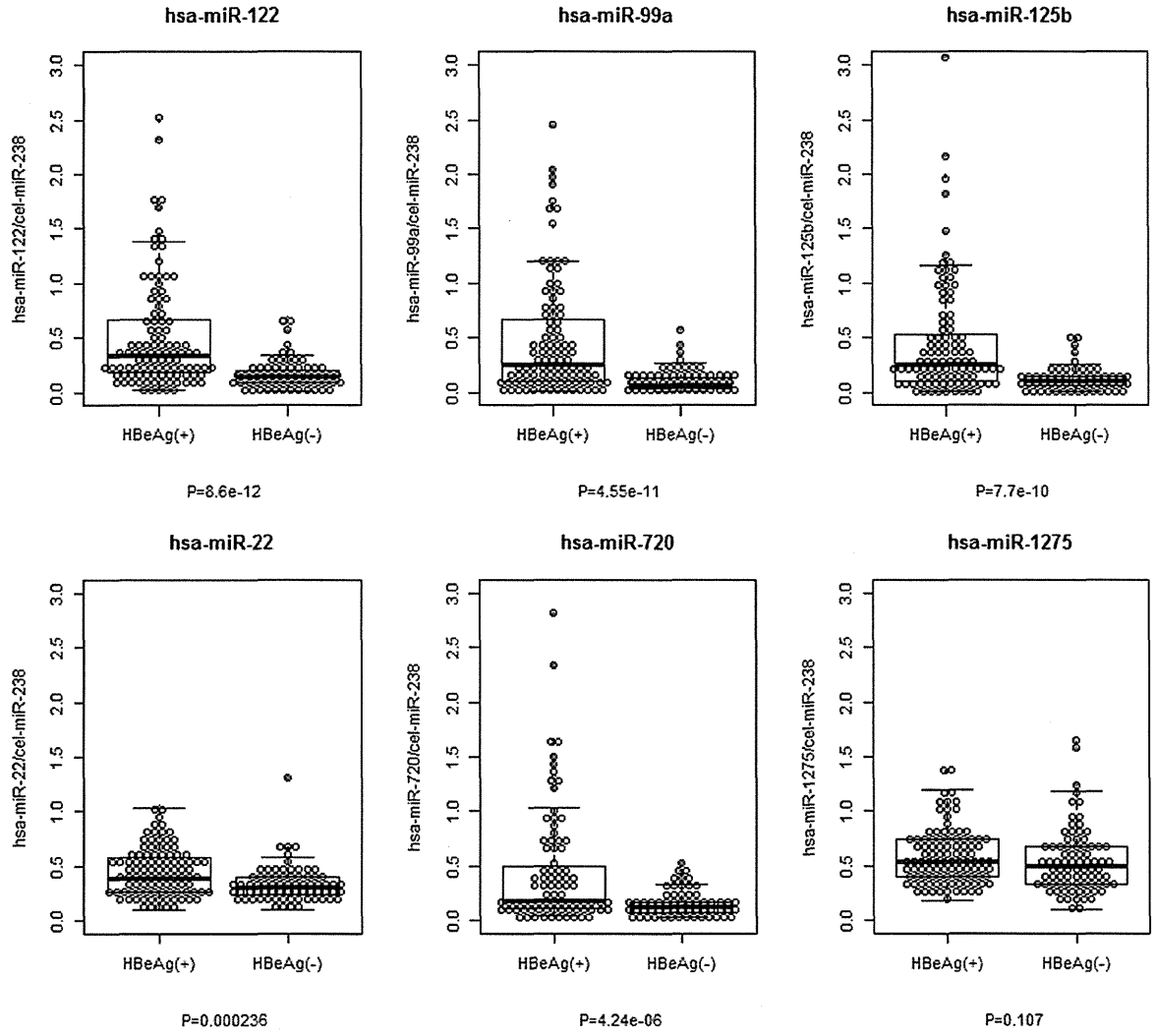

Figure 2 Serum microRNA expression in HBe antigen positive and negative individuals. qRT-PCR microRNA expression levels normalized by cel-miR-238 are shown. *P*-values represent the difference in median values using the non-parametric Kruskal–Wallis rank sum test.

qRT-PCR data (Table 5). MiR-122 was independently associated only with HBV DNA level, whereas miR-125b was independently associated with HBV DNA, HBsAg, HBeAg, and HBeAb levels. MiR-99a was also independently associated with HBeAb levels, and miR-720 was independently associated with HBsAg. While these microRNAs were associated with viral components, miR-22 and miR-1275 were independently associated with γGTP levels. rs8099917 SNP genotype TT in the IFNL3 locus was independently associated with necroinflammatory activity. MiR-125b was the strongest independent factor associated with HBeAg levels, and miR-125b and miR-99a and HBV DNA were each independently associated with HBeAg level. Pairwise expression levels of serum microRNAs were highly correlated, e.g., miR-22 and miR-99a (R^2 = 0.97), miR-99a and miR-125b (R^2 = 0.96), and miR-122 and miR-125b (R^2 = 0.96).

Pathway analysis

To determine which pathways HBV or HCV-associated microRNAs affected, gene targets were predicted using the miRWalk database, and predicted gene targets were compared against pathways in the Kyoto Encyclopedia of Genes and Genomes (KEGG) database. Predicted targets were found to be significantly overrepresented in the "Pathways in Cancer" gene set. Several of the genes in this set (*AKT1*, *AKT3*, *PTEN*, *BCL2*, *CDKN1B*, *CCND1*, and *TP53*) were also targeted by multiple microRNAs as part of a complex regulatory network. To further examine differences between HBV and HCV infection, predicted gene targets were analyzed using Ingenuity Pathway Analysis software. Significant associations were found between predicted targets and "Cancer," "Cell Cycle," and "Cell Death and Survival" networks in HCV patients and between

Table 5 Univariate and multivariate linear/logistic regression analysis of associations between clinical data and quantitative RT-PCR serum microRNA levels (relative to cel-miR-238) in patients with chronic HBV infection. Independent factors (bold) were determined using forward-backward stepwise selection based on the Akaike information criterion (AIC) using factors with a univariate *P*-value less than 0.05.

Variable	Factor	N	Coef.	P_{uni}	Coef.	P_{multi}	
HBV DNA (IU/ml)	**hsa-miR-122**	185	2.6	6.1E-17	3.8	7.43E-05	***
	hsa-miR-22	185	3.1	4.3E-06			
	hsa-miR-99a	185	2.3	3.7E-15			
	hsa-miR-720	185	1.5	4.0E-08	−0.5	1.08E-01	
	hsa-miR-125b	185	2.3	2.1E-13	−1.8	2.57E-02	*
	hsa-miR-1275	184	0.4	4.1E-01			
	HBsAg (IU/l)	185	0.0	6.7E-11			
	HBeAg (IU/l)	185	0.0	2.5E-13			
	HBeAb (+/−)	185	−2.2	1.8E-18	−1.5	9.76E-10	***
	rs8099917 TT	167	0.8	5.0E-03			
	AST	185	0.0	4.2E-04	0.0	6.60E-02	.
	ALT	185	0.0	7.4E-04			
	γ-GTP(IU/l)	179	0.0	2.3E-01			
	Liver fibrosis	171	0.2	3.8E-01			
	Activity	171	0.9	4.0E-06	0.6	2.00E-05	***
	Genotype C	145	−0.3	5.4E-01			
HBsAg (IU/l)	hsa-miR-122	185	62950.0	7.6E-60			
	hsa-miR-22	185	59425.0	1.1E-08			
	hsa-miR-99a	185	60936.0	6.9E-66			
	hsa-miR-720	185	41920.0	5.1E-31	14228.0	4.47E-08	***
	hsa-miR-125b	185	62707.0	9.0E-62	51193.0	7.20E-39	***
	hsa-miR-1275	184	2856.0	7.2E-01			
	HBeAg (IU/l)	185	34.0	3.6E-18			
	HBeAb (+/−)	185	−25347.0	1.7E-09			
	rs8099917 TT	167	12077.0	1.2E-02			
	HBV DNA (IU/ml)	185	7119.0	6.7E-11			
	AST	185	−10.3	6.6E-01			
	ALT	185	1.2	9.1E-01			
	γ-GTP	179	−12.6	7.3E-01			
	Liver fibrosis	171	−5283.0	8.4E-02			
	Activity	171	3301.0	3.1E-01			
	Genotype C	145	−16648.0	4.3E-02			
HBeAg (IU/l)	hsa-miR-122	185	751.0	2.8E-20			
	hsa-miR-22	185	872.0	1.3E-06			
	hsa-miR-99a	185	700.0	1.7E-19			
	hsa-miR-720	185	464.0	2.1E-11			
	hsa-miR-125b	185	741.0	3.4E-20	544.0	4.90E-13	***
	hsa-miR-1275	184	101.0	4.6E-01			
	HBsAg (IU/l)	185	0.0	3.6E-18			
	HBeAb (+/−)	185	−609.0	3.8E-19	−395.0	3.14E-10	***
	rs8099917 TT	167	121.0	1.4E-01			
	HBV DNA (IU/ml)	185	135.0	2.5E-13			
	AST	185	0.9	3.3E-02	0.6	3.50E-02	*
	ALT	185	0.4	2.2E-02			
	γ-GTP	179	0.4	5.3E-01			
	Liver fibrosis	171	−22.3	6.7E-01			
	Activity	171	94.1	9.2E-02			
	Genotype C	145	−1.5	9.9E-01			
HBeAb (+/−)	hsa-miR-122	184	−52.1	1.0E-12			
	hsa-miR-22	184	−65.8	2.4E-05			
	hsa-miR-99a	184	−49.8	7.4E-13	−55.3	3.90E-03	**
	hsa-miR-720	184	−32.2	1.3E-07			
	hsa-miR-125b	184	−46.4	2.6E-10	51.3	9.53E-03	**

Table 5 (*continued*)

Variable	Factor	N	Coef.	P_{uni}	Coef.	P_{multi}	
	hsa-miR-1275	183	−19.4	9.6E-02			
	HBsAg (IU/l)	184	0.0	1.3E-10			
	HBeAg (IU/l)	184	−0.1	7.4E-18	0.0	8.67E-07	***
	rs8099917 TT	166	−10.6	1.2E-01			
	HBV DNA (IU/ml)	184	−13.9	5.4E-20	−8.7	2.84E-08	***
	AST	184	−0.1	8.4E-02			
	ALT	184	0.0	2.9E-02			
	γ-GTP	178	0.0	6.9E-01			
	Liver fibrosis	170	−1.2	7.8E-01			
	Activity	170	−3.9	4.1E-01			
	Genotype C	144	−11.4	3.3E-01			
ALT (IU/l)	hsa-miR-122	185	17.0	6.3E-01			
	hsa-miR-22	185	337.0	1.0E-06	48.2	1.29E-01	
	hsa-miR-99a	185	−18.8	5.7E-01			
	hsa-miR-720	185	15.5	5.8E-01			
	hsa-miR-125b	185	−1.6	9.6E-01			
	hsa-miR-1275	184	9.0	8.6E-01			
	HBsAg (IU/l)	185	0.0	9.1E-01			
	HBeAg (IU/l)	185	0.1	2.2E-02			
	rs8099917 TT	167	18.2	5.5E-01			
	HBV DNA (IU/ml)	185	25.1	7.4E-04			
	AST	185	1.9	2.6E-66	1.8	2.20E-47	***
	γ-GTP	179	2.0	2.1E-20	0.4	6.05E-04	***
	Liver fibrosis	171	35.8	7.6E-02			
	Activity	171	74.8	4.3E-04	−19.0	4.58E-02	*
	Genotype C	145	30.0	5.6E-01			
AST (IU/l)	hsa-miR-122	185	0.2	9.9E-01			
	hsa-miR-22	185	148.0	8.2E-06			
	hsa-miR-99a	185	−15.1	3.4E-01			
	hsa-miR-720	185	4.1	7.6E-01			
	hsa-miR-125b	185	−7.3	6.6E-01			
	hsa-miR-1275	184	10.3	6.8E-01			
	HBsAg (IU/l)	185	0.0	6.6E-01			
	HBeAg (IU/l)	185	0.0	3.3E-02			
	rs8099917 TT	167	18.3	2.0E-01			
	HBV DNA (IU/ml)	185	12.6	4.2E-04			
	ALT	185	0.4	2.6E-66	0.4	1.05E-59	***
	γ-GTP	179	0.9	8.1E-18			
	Liver fibrosis	171	27.2	4.8E-03			
	Activity	171	48.6	1.5E-06	17.4	1.98E-04	***
	Genotype C	145	4.0	8.7E-01			
γ-GTP (IU/l)	hsa-miR-122	179	−5.3	6.4E-01			
	hsa-miR-22	179	46.4	4.2E-02	−48.0	1.95E-02	*
	hsa-miR-99a	179	−10.1	3.4E-01			
	hsa-miR-720	179	3.9	6.7E-01			
	hsa-miR-125b	179	−9.7	3.8E-01			
	hsa-miR-1275	178	33.9	4.3E-02	43.2	2.70E-03	**
	HBsAg (IU/l)	179	0.0	7.3E-01			
	HBeAg (IU/l)	179	0.0	5.3E-01			
	rs8099917 TT	161	10.9	2.7E-01			
	HBV DNA (IU/ml)	179	3.0	2.3E-01			
	AST	179	0.4	8.1E-18			
	ALT	179	0.2	2.1E-20	0.2	5.35E-19	***
	Liver fibrosis	166	24.1	1.7E-04	15.9	1.59E-03	**
	Activity	166	23.5	7.4E-04			
	Genotype C	140	15.7	3.3E-01			

(*continued on next page*)

Table 5 (*continued*)

Variable	Factor	N	Coef.	P_{uni}	Coef.	P_{multi}	
Liver fibrosis	hsa-miR-122	171	−0.3	6.4E-02			
	hsa-miR-22	171	0.0	9.3E-01			
	hsa-miR-99a	171	−0.3	5.3E-02			
	hsa-miR-720	171	−0.1	4.6E-01			
	hsa-miR-125b	171	−0.2	7.7E-02			
	hsa-miR-1275	170	0.2	2.6E-01			
	HBsAg (IU/l)	171	0.0	8.4E-02			
	HBeAg (IU/l)	171	0.0	6.7E-01			
	rs8099917 TT	160	0.4	1.8E-04			
	HBV DNA (IU/ml)	171	0.0	3.8E-01			
	AST	171	0.0	4.8E-03			
	ALT	171	0.0	7.6E-02			
	γ-GTP	166	0.0	1.7E-04	0.0	3.79E-02	*
	Activity	171	0.6	4.8E-15	0.5	1.35E-09	***
	Genotype C	139	0.4	3.0E-02	0.4	2.63E-02	*
Activity	hsa-miR-122	171	0.2	1.6E-01			
	hsa-miR-22	171	0.4	1.3E-01			
	hsa-miR-99a	171	0.2	1.7E-01			
	hsa-miR-720	171	0.2	1.4E-01			
	hsa-miR-125b	171	0.2	1.1E-01			
	hsa-miR-1275	170	0.1	7.4E-01			
	HBsAg (IU/l)	171	0.0	3.1E-01			
	HBeAg (IU/l)	171	0.0	9.2E-02			
	rs8099917 TT	160	0.9	1.9E-17	0.6	3.80E-13	***
	HBV DNA	171	0.1	4.0E-06	0.1	1.51E-03	**
	AST	171	0.0	1.5E-06	0.0	5.66E-04	***
	ALT	171	0.0	4.3E-04			
	γ-GTP	166	0.0	7.4E-04			
	Liver fibrosis	171	0.5	4.8E-15	0.4	7.00E-11	***
	Genotype C	139	0.0	8.1E-01			

predicted targets and "Cancer," "Hematological Disease," and "Gastrointestinal Disease" networks in HBV patients. To determine if the HBV-associated serum microRNAs shared common transcriptional regulators, upstream transcription factors for each up-regulated microRNA were retrieved from ChIPBase (http://deepbase.sysu.edu.cn/chipbase/ accessed on 14 September 2014).[23] NRSF, JunD, c-Jun transcription have been reported to regulate expression of miR-125b, miR-22, and miR-99a. ZNF11 regulates both miR-125b and miR-99a, and NANOG, E2F4, and HNF4A have been reported to regulate miR-122 and miR-22.

Discussion

This study reports a set of microRNAs that were up- or down-regulated in serum of patients with chronic HBV or HCV compared to healthy subjects. MiR-122 was significantly up-regulated in serum of patients with HBV or HCV, whereas elevated miR-22, miR-99, and miR-125b levels were more characteristic of chronic HBV infection. A number of microRNAs were up-regulated in HBeAg-positive patients compared to HBeAg-negative patients. The HBeAg-associated microRNAs are regulated by a small set of shared transcription factors, including c-Jun, ZNF11, and HNF4A.[23] Expression levels of most HBeAg-associated microRNAs were highly correlated, but individual microRNAs were independently associated with different aspects of HBV infection. MiR-122 was independently associated with HBV DNA, whereas miR-125b was associated with multiple aspects of viral replication, including HBV DNA, HBsAg, and HBeAg, and miR-22 and miR-1275 were independently associated with serum levels of γGTP, a liver enzyme normally associated with alcoholic liver disease or biliary obstruction but which may be elevated in the event of severe viral hepatitis.[24] These results suggest that serum microRNA profiles might serve a diagnostic role in monitoring different aspects of viral infection, although their specific roles in pathogenesis of viral hepatitis remain to be worked out.

The presence of specific serum microRNA profiles associated with chronic HCV or HBV infection suggests involvement of these microRNAs in host-mediated antiviral defense or pathogenesis. Hepatic microRNAs enter the serum via apoptosis or necrosis, or they may be actively secreted within exosomes or viral particles.[14] MiR-122 is abundantly expressed in hepatocytes, and its presence in the serum has been shown to correlate with ALT levels and liver damage.[25,26] MiR-122 strongly suppresses HBV replication both through direct binding to HBV RNA as well as indirectly through cyclin G1-modulated p53 activity.[27–31] MiR-125a-5p, miR-199a-3p and miR-210 also

inhibit viral replication by directly binding to and suppressing HBV RNA.[30,32,33] MiR-99a is abundantly expressed in the liver and in exosomes and acts as a tumor suppressor by targeting IGF-1R and inducing cell cycle arrest.[16,34] In addition, miR-99 suppresses activity of NF-κB, a transcription factor associated with inflammation and tumorigenesis.[35] In HCC, miR-99a may be severely down-regulated in liver tissue, which is associated with poor prognosis and shorter survival time.[34] As with miR-99a, miR-22 is also abundantly expressed in hepatocytes and exosomes and acts as a tumor suppressor.[16] MiR-22 induces cellular senescence by directly targeting CDKN1A, CDK6, SIRT1, and Sp1 HCC[36,37] and is down-regulated in HBV-related HCC.[37]

Two serum microRNAs investigated in this study (miR-1246 and miR-1275) are part of a set of 13 mitomiRs that have been reported to be significantly enriched in the mitochondrial RNA fraction.[38] Mitochondria play a central role in oxidative stress and apoptosis and are targeted by the HBV X (HBx) protein and the HCV p7 protein.[39] Most mitomiRs, including miR-1246 and miR-1275, are predicted to target COX1, ND5, or other components of the respiratory chain.[38] In this study miR-1275 was significantly up-regulated in patients with HBV and was independently associated with γGTP level, whereas miR-1246 was marginally up-regulated in patients with HCV. MiR-720 has been reported to target the oncogene TWIST1 involved in tumor metastasis in breast cancer,[40] but its status as a microRNA has been challenged due to a possible mis-annotation of what may be a tRNA fragment instead.[41]

An unexpected result of this study is that serum levels of a number of microRNAs were elevated in HBeAg-positive patients compared to HBeAg-negative patients, even though expression levels of both HBeAg-positive and negative patients were both higher than in healthy subjects. The role of the HBe antigen in HBV infection remains unclear, as it is not required for infection but may serve an immunomodulatory role and contribute to chronic infection through vertical transmission by crossing the placenta. However, the HBV precore region that codes for the HBe antigen is highly conserved among hepadnaviruses, which also infect avian hosts lacking a placenta, suggesting that the protein has a more fundamental function. The precore protein contains a signal peptide, causing it to be secreted.[42] However, up to 30% of the protein is retained in the cytoplasm.[43] While secreted HBeAg may have an immunosuppressive role, intracellular HBeAg instead promotes inflammation.[44] However, HBeAg has been shown to inhibit Toll-like receptor signaling and suppress NF-kB and interferon-beta promoter activity.[45] HBeAg also inhibits IL-6 production by blocking activation of RIPK2-mediated activation of NF-kB.[46] Therefore HBeAg may have a complex roles in both intracellular and extracellular immune modulation.

Seroconversion of HBeAg-positive patients to HBe antibody (HBeAb)-positive patients is usually accompanied by a stop codon mutation within the precore open reading frame.[47] This region has been identified as a mutation hotspot for APOBEC3G, an interferon-stimulated deaminase that inhibits HBV replication by hyper-editing of single-stranded HBV DNA[22] as well as by directly blocking reverse transcription.[48] While hypermutation is deleterious to the virus, a small fraction may acquire mutations conferring a selective advantage.[22] Warner et al. proposed a frequency-dependent selection model positing that while HBeAg suppresses the immune response, HBeAg-negative strains may have an initial competitive advantage by benefitting from HBeAg-mediated immune suppression conferred by HBeAg-positive strains while expending fewer of its resources.[49] However, as the frequency of the HBeAg-positive strain falls, the immune system begins to mount a defense against HBeAg-negative viruses, leading to seroconversion.

It is not clear why serum microRNA levels of several microRNAs, including miR-122, miR-22, miR-125, and miR-99a, tended to be higher in HBeAg-positive individuals compared to HBeAg-negative individuals and are higher in HBV-infected individuals compared to healthy subjects. However, Winther et al. reported similar results in children with chronic hepatitis B and found that plasma levels of a subset of microRNAs decreased significantly in one child before and after HBe seroconversion.[50] We have previously shown that both HBc and HBs proteins co-localize and physically interact with AGO2 in hepatocytes and that siRNA ablation of AGO2 suppressed HBV DNA and HBsAg production,[10] suggesting that components of the RNA silencing machinery are recruited during HBV replication. HSP90 has been reported to act as a chaperone during RNA loading of Argonaute proteins[51] and is also essential in catalyzing HBV reverse transcription and capsid formation by interacting with the pregenomic RNA encapsidation signal, reverse transcriptase, and the core protein.[52] Interestingly, APOBEC3G has been shown to interfere with microRNA regulation by disrupting assembly of the miRNA-inducing silencing complex (miRISC).[53] APOBEC3G itself is also incorporated into nucleocapsids by directly binding to the core protein.[54] While microRNA-mediated gene silencing is associated with accumulation in P-bodies, microRNAs may also be sorted into multivesicular bodies by ESCRT proteins and secreted as exosomes.[55] MiR-122, miR-125b, miR-199a, miR-210, and possibly other microRNAs bind directly to targets within the HBV genome. MiR-199a and miR-210 have been shown to suppress HBsAg production in cell culture. However, HBV has been shown to enhance autophagy without a corresponding increase in protein degradation by HBsAg-mediated activation of the unfolded protein response, and disruption of autophagy inhibits HBV production.[56] Although it is not clear how or if HBeAg is involved in this process, it is possible that the loss of non-secreted intracellular HBeAg or a conformational change in precore RNA resulting from precore mutations interferes with viral control of autophagy or suppression of innate immune signaling. This loss of control over the intracellular environment might result in suppressed viral replication and decreased secretion of exosome-associated microRNAs.

The millions of people chronically infected with HBV or HCV pose a serious public health challenge. While cirrhosis and HCC may develop over a span of decades, HCC is often not detected until late in development, resulting in poor prognosis and leaving few treatment options. Sensitive, non-invasive methods able to detect subtle changes in disease state are needed for early identification of individuals at increased risk. Serum microRNAs may improve

early detection by providing an indirect means to monitor changes in gene and microRNA expression in the liver.

Conflicts of interest

None.

Acknowledgments

This work was supported by Grants-in-Aid for scientific research and development from the Ministry of Health, Labor and Welfare and Ministry of Education Culture Sports Science and Technology, Government of Japan. No writing assistance was provided for this manuscript.

Appendix A. Supplementary data

Supplementary data related to this article can be found at doi:10.1016/j.jinf.2014.10.017.

References

1. Fields BN, Knipe DM, Howley PM. *Fields virology*. 5th ed. Philadelphia: Wolters Kluwer Health/Lippincott Williams & Wilkins; 2007.
2. McMahon BJ. The natural history of chronic hepatitis B virus infection. *Hepatology* 2009 May;**49**(5 Suppl):S45–55 [Consensus Development Conference, NIH Research Support, U.S. Gov't, P.H.S.].
3. Brechot C, Kremsdorf D, Soussan P, Pineau P, Dejean A, Paterlini-Brechot P, et al. Hepatitis B virus (HBV)-related hepatocellular carcinoma (HCC): molecular mechanisms and novel paradigms. *Pathol Biol (Paris)* 2010 Aug;**58**(4):278–87 [Review].
4. Xi Y, Nakajima G, Gavin E, Morris CG, Kudo K, Hayashi K, et al. Systematic analysis of microRNA expression of RNA extracted from fresh frozen and formalin-fixed paraffin-embedded samples. *RNA* 2007 Oct;**13**(10):1668–74 [Research Support, N.I.H., Extramural].
5. Liu AM, Zhang C, Burchard J, Fan ST, Wong KF, Dai H, et al. Global regulation on microRNA in hepatitis B virus-associated hepatocellular carcinoma. *Omics* 2011 Mar;**15**(3):187–91.
6. Bala S, Marcos M, Szabo G. Emerging role of microRNAs in liver diseases. *World J Gastroenterol* 2009 Dec 7;**15**(45):5633–40 [Research Support, N.I.H., Extramural Research Support, Non-U.S. Gov't Review].
7. Ji F, Yang B, Peng X, Ding H, You H, Tien P. Circulating microRNAs in hepatitis B virus-infected patients. *J Viral Hepat* 2011 Jul;**18**(7):e242–51 [Research Support, Non-U.S. Gov't].
8. Mitchell PS, Parkin RK, Kroh EM, Fritz BR, Wyman SK, Pogosova-Agadjanyan EL, et al. Circulating microRNAs as stable blood-based markers for cancer detection. *Proc Natl Acad Sci U. S. A.* 2008 Jul 29;**105**(30):10513–8 [Research Support, N.I.H., Extramural Research Support, Non-U.S. Gov't].
9. Ura S, Honda M, Yamashita T, Ueda T, Takatori H, Nishino R, et al. Differential microRNA expression between hepatitis B and hepatitis C leading disease progression to hepatocellular carcinoma. *Hepatology* 2009 Apr;**49**(4):1098–112.
10. Hayes CN, Akamatsu S, Tsuge M, Miki D, Akiyama R, Abe H, et al. Hepatitis B virus-specific miRNAs and argonaute2 play a role in the viral life cycle. *PLoS One* 2012;**7**(10):e47490 [Research Support, Non-U.S. Gov't].
11. Shwetha S, Gouthamchandra K, Chandra M, Ravishankar B, Khaja MN, Das S. Circulating miRNA profile in HCV infected serum: novel insight into pathogenesis. *Sci Rep* 2013 Apr;3(3):1555 [Research Support, Non-U.S. Gov't].
12. Turchinovich A, Weiz L, Langheinz A, Burwinkel B. Characterization of extracellular circulating microRNA. *Nucleic Acids Res* 2011 Sep 1;39(16):7223–33 [Research Support, Non-U.S. Gov't].
13. Arroyo JD, Chevillet JR, Kroh EM, Ruf IK, Pritchard CC, Gibson DF, et al. Argonaute2 complexes carry a population of circulating microRNAs independent of vesicles in human plasma. *Proc Natl Acad Sci U. S. A* 2011 Mar 22;**108**(12):5003–8 [Research Support, N.I.H., Extramural Research Support, Non-U.S. Gov't].
14. Novellino L, Rossi RL, Bonino F, Cavallone D, Abrignani S, Pagani M, et al. Circulating hepatitis B surface antigen particles carry hepatocellular microRNAs. *PLoS One* 2012;**7**(3):e31952.
15. Gallo A, Tandon M, Alevizos I, Illei GG. The majority of microRNAs detectable in serum and saliva is concentrated in exosomes. *PLoS One* 2012;**7**(3):e30679 [Comparative Study Research Support, N.I.H., Intramural].
16. Huang X, Yuan T, Tschannen M, Sun Z, Jacob H, Du M, et al. Characterization of human plasma-derived exosomal RNAs by deep sequencing. *BMC Genomics* 2013;**14**:319 [Research Support, N.I.H., Extramural Research Support, Non-U.S. Gov't].
17. Conde-Vancells J, Rodriguez-Suarez E, Embade N, Gil D, Matthiesen R, Valle M, et al. Characterization and comprehensive proteome profiling of exosomes secreted by hepatocytes. *J Proteome Res* 2008 Dec;**7**(12):5157–66 [Research Support, N.I.H., Extramural Research Support, Non-U.S. Gov't].
18. Li J, Liu K, Liu Y, Xu Y, Zhang F, Yang H, et al. Exosomes mediate the cell-to-cell transmission of IFN-alpha-induced antiviral activity. *Nat Immunol* 2013 Aug;**14**(8):793–803 [Research Support, Non-U.S. Gov't].
19. Desmet VJ, Gerber M, Hoofnagle JH, Manns M, Scheuer PJ. Classification of chronic hepatitis: diagnosis, grading and staging. *Hepatology* 1994 Jun;**19**(6):1513–20 [Review].
20. Dweep H, Sticht C, Pandey P, Gretz N. miRWalk–database: prediction of possible miRNA binding sites by "walking" the genes of three genomes. *J Biomed Inf* 2011 Oct;**44**(5):839–47 [Research Support, Non-U.S. Gov't].
21. Mathivanan S, Fahner CJ, Reid GE, Simpson RJ. ExoCarta 2012: database of exosomal proteins, RNA and lipids. *Nucleic Acids Res* 2012 Jan;**40**(Database issue):D1241–4 [Research Support, Non-U.S. Gov't].
22. Vartanian JP, Henry M, Marchio A, Suspene R, Aynaud MM, Guetard D, et al. Massive APOBEC3 editing of hepatitis B viral DNA in cirrhosis. *PLoS Pathog* 2010 May;**6**(5):e1000928 [Research Support, Non-U.S. Gov't].
23. Yang JH, Li JH, Jiang S, Zhou H, Qu LH. ChIPBase: a database for decoding the transcriptional regulation of long non-coding RNA and microRNA genes from ChIP-Seq data. *Nucleic Acids Res* 2013 Jan;**41**(Database issue):D177–87 [Research Support, Non-U.S. Gov't].
24. Lum G, Gambino SR. Serum gamma-glutamyl transpeptidase activity as an indicator of disease of liver, pancreas, or bone. *Clin Chem* 1972 Apr;**18**(4):358–62.
25. Bala S, Petrasek J, Mundkur S, Catalano D, Levin I, Ward J, et al. Circulating microRNAs in exosomes indicate hepatocyte injury and inflammation in alcoholic, drug-induced, and inflammatory liver diseases. *Hepatology* 2012 Nov;**56**(5):1946–57 [Research Support, N.I.H., Extramural].
26. Arataki K, Hayes CN, Akamatsu S, Akiyama R, Abe H, Tsuge M, et al. Circulating microRNA-22 correlates with microRNA-122

and represents viral replication and liver injury in patients with chronic hepatitis B. *J Med Virology* 2013 May;**85**(5): 789–98 [Research Support, Non-U.S. Gov't].
27. Wang S, Qiu L, Yan X, Jin W, Wang Y, Chen L, et al. Loss of MiR-122 expression in patients with hepatitis B enhances hepatitis B virus replication through cyclin G1 modulated P53 activity. *Hepatology* 2012 Mar;**55**(3):730–41.
28. Hu J, Xu Y, Hao J, Wang S, Li C, Meng S. MiR-122 in hepatic function and liver diseases. *Protein Cell* 2012 May;**3**(5): 364–71.
29. Chang J, Nicolas E, Marks D, Sander C, Lerro A, Buendia MA, et al. miR-122, a mammalian liver-specific microRNA, is processed from hcr mRNA and may downregulate the high affinity cationic amino acid transporter CAT-1. *RNA Biol* 2004 Jul;**1**(2): 106–13 [Research Support, N.I.H., Extramural Research Support, Non-U.S. Gov't].
30. Chen Y, Shen A, Rider PJ, Yu Y, Wu K, Mu Y, et al. A liver-specific microRNA binds to a highly conserved RNA sequence of hepatitis B virus and negatively regulates viral gene expression and replication. *Faseb J* 2011 Dec;**25**(12):4511–21.
31. Qiu L, Fan H, Jin W, Zhao B, Wang Y, Ju Y, et al. miR-122-induced down-regulation of HO-1 negatively affects miR-122-mediated suppression of HBV. *Biochem Biophys Res Commun* 2010 Aug 6;**398**(4):771–7 [Research Support, Non-U.S. Gov't].
32. Potenza N, Papa U, Mosca N, Zerbini F, Nobile V, Russo A. Human microRNA hsa-miR-125a-5p interferes with expression of hepatitis B virus surface antigen. *Nucleic Acids Res* 2011 Jul; **39**(12):5157–63.
33. Zhang GL, Li YX, Zheng SQ, Liu M, Li X, Tang H. Suppression of hepatitis B virus replication by microRNA-199a-3p and microRNA-210. *Antivir Res* 2010 Nov;**88**(2):169–75 [Research Support, Non-U.S. Gov't].
34. Li D, Liu X, Lin L, Hou J, Li N, Wang C, et al. MicroRNA-99a inhibits hepatocellular carcinoma growth and correlates with prognosis of patients with hepatocellular carcinoma. *J Biol Chem* 2011 Oct 21;**286**(42):36677–85 [Research Support, Non-U.S. Gov't].
35. Takata A, Otsuka M, Kojima K, Yoshikawa T, Kishikawa T, Yoshida H, et al. MicroRNA-22 and microRNA-140 suppress NF-kappaB activity by regulating the expression of NF-kappaB coactivators. *Biochem Biophys Res Commun* 2011 Aug 12;**411**(4):826–31 [Research Support, Non-U.S. Gov't].
36. Xu D, Takeshita F, Hino Y, Fukunaga S, Kudo Y, Tamaki A, et al. miR-22 represses cancer progression by inducing cellular senescence. *J Cell Biol* 2011 Apr 18;**193**(2):409–24 [Research Support, Non-U.S. Gov't].
37. Shi C, Xu X. MicroRNA-22 is down-regulated in hepatitis B virus-related hepatocellular carcinoma. *Biomed Pharmacother* 2013 Jun;**67**(5):375–80 [Research Support, Non-U.S. Gov't].
38. Bandiera S, Ruberg S, Girard M, Cagnard N, Hanein S, Chretien D, et al. Nuclear outsourcing of RNA interference components to human mitochondria. *PLoS One* 2011;**6**(6): e20746.
39. D'Agostino DM, Bernardi P, Chieco-Bianchi L, Ciminale V. Mitochondria as functional targets of proteins coded by human tumor viruses. *Adv Cancer Res* 2005;**94**:87–142.
40. Li LZ, Zhang CZ, Liu LL, Yi C, Lu SX, Zhou X, et al. miR-720 inhibits tumor invasion and migration in breast cancer by targeting TWIST1. *Carcinogenesis* 2014 Feb;**35**(2):469–78 [Comparative Study Research Support, Non-U.S. Gov't].
41. Schopman NC, Heynen S, Haasnoot J, Berkhout B. A miRNA-tRNA mix-up: tRNA origin of proposed miRNA. *RNA Biol* 2010 Sep-Oct;**7**(5):573–6 [Research Support, Non-U.S. Gov't].
42. Ou JH, Laub O, Rutter WJ. Hepatitis B virus gene function: the precore region targets the core antigen to cellular membranes and causes the secretion of the e antigen. *Proc Natl Acad Sci U. S. A* 1986 Mar;**83**(6):1578–82 [Research Support, U.S. Gov't, P.H.S.].
43. Garcia PD, Ou JH, Rutter WJ, Walter P. Targeting of the hepatitis B virus precore protein to the endoplasmic reticulum membrane: after signal peptide cleavage translocation can be aborted and the product released into the cytoplasm. *J Cell Biol* 1988 Apr;**106**(4):1093–104 [Research Support, Non-U.S. Gov't Research Support, U.S. Gov't, P.H.S.].
44. Milich D, Liang TJ. Exploring the biological basis of hepatitis B e antigen in hepatitis B virus infection. *Hepatology* 2003 Nov; **38**(5):1075–86 [Review].
45. Lang T, Lo C, Skinner N, Locarnini S, Visvanathan K, Mansell A. The hepatitis B e antigen (HBeAg) targets and suppresses activation of the toll-like receptor signaling pathway. *J Hepatol* 2011 Oct;**55**(4):762–9 [Research Support, Non-U.S. Gov't].
46. Wu S, Kanda T, Imazeki F, Nakamoto S, Tanaka T, Arai M, et al. Hepatitis B virus e antigen physically associates with receptor-interacting serine/threonine protein kinase 2 and regulates IL-6 gene expression. *J Infect Dis* 2012 Aug 1; **206**(3):415–20 [Research Support, Non-U.S. Gov't].
47. Tong S, Kim KH, Chante C, Wands J, Li J. Hepatitis B Virus e Antigen Variants. *Int J Med Sci* 2005;**2**(1):2–7.
48. Nguyen DH, Hu J. Reverse transcriptase- and RNA packaging signal-dependent incorporation of APOBEC3G into hepatitis B virus nucleocapsids. *J Virol* 2008 Jul;**82**(14):6852–61 [Research Support, N.I.H., Extramural].
49. Warner BG, Abbott WG, Rodrigo AG. Frequency-dependent selection drives HBeAg seroconversion in chronic hepatitis B virus infection. *Evol Med Public Health* 2014 Jan;**2014**(1): 1–9.
50. Winther TN, Bang-Berthelsen CH, Heiberg IL, Pociot F, Hogh B. Differential plasma microRNA profiles in HBeAg positive and HBeAg negative children with chronic hepatitis B. *PLoS One* 2013;**8**(3):e58236 [Research Support, Non-U.S. Gov't].
51. Johnston M, Geoffroy MC, Sobala A, Hay R, Hutvagner G. HSP90 protein stabilizes unloaded argonaute complexes and microscopic P-bodies in human cells. *Mol Biol Cell* 2010 May 1;**21**(9):1462–9 [Research Support, Non-U.S. Gov't].
52. Shim HY, Quan X, Yi YS, Jung G. Heat shock protein 90 facilitates formation of the HBV capsid via interacting with the HBV core protein dimers. *Virology* 2011 Feb 5;**410**(1):161–9 [Research Support, Non-U.S. Gov't].
53. Liu C, Zhang X, Huang F, Yang B, Li J, Liu B, et al. APOBEC3G inhibits microRNA-mediated repression of translation by interfering with the interaction between Argonaute-2 and MOV10. *J Biol Chem* 2012 Aug 24;**287**(35):29373–83 [Research Support, N.I.H., Extramural sResearch Support, Non-U.S. Gov't].
54. Zhao D, Wang X, Lou G, Peng G, Li J, Zhu H, et al. APOBEC3G directly binds Hepatitis B virus core protein in cell and cell free systems. *Virus Res* 2010 Aug;**151**(2):213–9 [Research Support, Non-U.S. Gov't].
55. Gibbings DJ, Ciaudo C, Erhardt M, Voinnet O. Multivesicular bodies associate with components of miRNA effector complexes and modulate miRNA activity. *Nat Cell Biol* 2009 Sep; **11**(9):1143–9 [Comment Research Support, Non-U.S. Gov't].
56. Li J, Liu Y, Wang Z, Liu K, Wang Y, Liu J, et al. Subversion of cellular autophagy machinery by hepatitis B virus for viral envelopment. *J Virol* 2011 Jul;**85**(13):6319–33 [Research Support, Non-U.S. Gov't].

Journal of Gastroenterology and Hepatology

JGHF

doi:10.1111/jgh.12715

HEPATOLOGY

The effects of bisphosphonate zoledronic acid in hepatocellular carcinoma, depending on mevalonate pathway

Yohji Honda, Shoichi Takahashi, Yizhou Zhang, Atsushi Ono, Eisuke Murakami, Niu Shi, Tomokazu Kawaoka, Daiki Miki, Masataka Tsuge, Nobuhiko Hiraga, Hiromi Abe, Hidenori Ochi, Michio Imamura, Hiroshi Aikata and Kazuaki Chayama

Department of Medicine and Molecular Science, Hiroshima University, Hiroshima, Japan

Key words
apoptosis, bisphosphonate, Ras and RhoA, zoledronic acid.

Accepted for publication 8 August 2014.

Correspondence
Dr Shoichi Takahashi, Department of Medicine and Molecular Science, Graduate School of Biomedical Sciences, Hiroshima University, 1-2-3 Kasumi, Minamiku, Hiroshima 734-8551, Japan. Email shoichit@hiroshima-u.ac.jp

Declaration of conflicts of interest: All authors declare no conflict of interest.

Abstract

Background and Aim: Zoledronic acid (ZOL) is a nitrogen-containing bisphosphonate and is used to reduce cancer-induced osteolysis. We reported previously that ZOL delayed both the growth and pain progression of bone metastases from hepatocellular carcinoma. The present study was designed to evaluate the effects of ZOL on hepatoma cell lines and the molecular mechanisms of such effects.

Methods: Cell viability assay, scratch assay, immunohistochemistry, Western blotting, and flow cytometry analysis were performed using Huh7 and HepG2 cells treated with and without ZOL.

Results: ZOL reduced cell growth in a dose-dependent manner and prevented cell migration when used at a concentration exceeding 10 μM. Immunohistochemistry showed that the inhibitory effects of ZOL on hepatoma cell progression was not due to the suppression of Ras and RhoA expression but due to inhibition of their translocation from the cytosol to the cell membrane, which terminates mevalonate pathway. Immunoblotting and flow cytometry showed that ZOL inhibited the mitogen-activated protein kinase pathway (MAPK) and induced apoptosis of hepatoma cells.

Conclusions: Our results indicated that ZOL prevented cell growth and metastasis based on direct antitumor effects in hepatoma cells. The use of ZOL could not only suppress the progression to bone metastatic lesions but also prevented growth of primary hepatocellular carcinoma.

Introduction

Hepatocellular carcinoma (HCC) is one of the most common cancers and is a leading cause of cancer death worldwide.[1–3] Hepatitis C (HCV) and B viruses (HBV) cause chronic infection, and 300 million and 170 million people suffer from chronic hepatitis or liver cirrhosis, respectively. Among these, more than 700 000 people die annually from HCC worldwide. Therefore, the development of new diagnostic and therapeutic modalities is desirable. Recently, the prognosis of such patients and those with HCC has improved.[4–6] However, this improvement has eventually increased the occurrence of extra-hepatic metastases from HCC. This is because among the patients who survive HCC with treatment, living cancer cells also survive in the peripheral circulation and thus have a larger chance to form distal metastasis. At present, bone metastasis is the second or third most frequent metastasis from HCC and 5.2–10.2% of HCC patients present with bone metastasis at diagnosis.[7–9] Unfortunately, bone metastasis in such patients is associated with severe pain.

Bisphosphonates (BPs) are inhibitors of bone-resorption. Among BPs, zoledronic acid (ZOL) is currently the strongest nitrogen-containing BP and is used for cancer-induced osteolysis to prevent skeletal complications associated with bone metastases. We reported previously that ZOL delays both the appearance and worsening of pain associated with bone metastases in patients with HCC.[10] Recent experimental *in vitro* studies have also indicated that ZOL acts directly on cancer cells, such as breast cancer cells, which metastasize easily to bones.[11–16] ZOL inhibits farnesyl pyrophosphate synthase, a key enzyme in the mevalonate pathway.[17,18] Accordingly, ZOL inhibits the prenylation of small G-proteins, such as Ras and RhoA, reduces the signals, and prevents the growth, adhesion, and migration of cancer cells. ZOL has high affinity for mineralized bone, with rapid localization into the bone, resulting in therapeutically effective local concentrations for cancer cells.

Apart from breast and prostate cancers, there is little or no information on the effects of ZOL in HCC at a molecular level, although it has already been used clinically for the treatment of

bone metastasis in HCC. In this study, we examined the effects of ZOL in hepatoma cell lines *in vitro*.

Methods

Cell culture. Human hepatoma cell lines Huh7 and HepG2 were used in this study. The cells were grown in William's Medium (Gibco BRL, Grand Island, NY, USA) supplemented with 10% fetal bovine serum (FBS), 10-mM 4-(2-hydroxyethyl)-1-piperazineethanesulfonic acid (HEPES), glutamax, and penicillin/streptomycin. ZOL was kindly provided by Novartis Pharmaceutical Company (Basel, Switzerland). Cells were cultured at 37°C in a humidified 5% CO_2 atmosphere. Then, adherent cells were incubated with the indicated concentrations of ZOL for the indicated time periods.

Cell proliferation. For the proliferation assay, we used the concentration of FBS (10%) to allow sufficient viability of Huh7 and HepG2 cells. Just after trypsinization, the cells were seeded at a concentration of 1×10^4 cells per well in a 96-well plate and incubated with ZOL for 24 h. Cell viability was measured 48 h later for Huh7 and HepG2 cells using the Cell Quanti-Blue Cell Viability Assay Kit (Bio Assay Systems, Hayward, CA, USA).

Cell migration. Cell migration was assembled according to the method of scratch assay.[19] Subconfluent growing cells were resuspended in type I collagen-coated six-well plate. The plate was incubated for approximately 6 h at 37°C, allowing cells to adhere, spread, and create a confluent monolayer on the substrate. Then, the cell monolayer was scraped in a straight line to create a "scratch" with a p200 pipette tip. The debris was removed and the edge of scratch was smoothed by washing the cells once with 1 mL of phosphate-buffered saline (PBS), then with a medium containing predetermined concentration of ZOL. The markings were pointed on the substrate near the scratch to obtain the same field, and the scratch was observed and recorded under a phase-contrast microscope (Olympus, Tokyo, Japan). The dish was placed in a tissue culture incubator at 37°C for more 18 h. The scratch was observed and recorded under a phase-contrast microscope again and compared under these two phases.

Separation of proteins. After incubation with ZOL at different concentration for 24 h, the proteins were separated using the following procedure. HCC cells were washed with cold PBS, lysed in ice-cold radioimmunoprecipitation assay (RIPA) buffer containing phosphatase and protease inhibitors and centrifuged at 15 000 rpm for 15 min at 4°C. The supernatant was collected as the full cell fraction. The protein concentration was determined by the method of Bradford using the Bio-Rad protein assay (Bio-Rad Laboratories, Inc., Hercules, CA, USA).

Immunoblotting analysis. The immunoprecipitated proteins were resuspended in loading buffer, boiled for 5 min at 99°C, and further subjected to electrophoresis on sodium dodecyl sulfate polyacrylamide gel. Equal amounts of protein extracts (50 μg) were subjected to polyacrylamide gel electrophoresis (PAGE) under denaturing conditions. Proteins were electrotransferred onto polyvinylidene difluoride membrane. Membranes were immunoblotted with primary antibodies overnight at 4°C with pan-Ras and RhoA polyclonal antibodies (dilution, 1:1000, from Cell Signaling Technology, Beverly, MA, USA), Erk1/2 and phospho-Erk1/2 (dilution, 1:1000, from Cell Signaling Technology), or Bak, Bax, Bcl-XL, MCL-1 monoclonal antibodies (dilution, 1:1000, from Cell Signaling Technology), followed by incubation with the appropriate mouse or rabbit derived secondary antibody at room temperature for 1 h and developed with electrochemiluminescence (ECL) solution (Amersham Pharmacia Biotech, Piscataway, NJ, USA) and exposed to Kodak X-OMAT films (Sigma-Aldrich Corporation, St. Louis, MO, USA). Blots were rehybridized with β-actin polyclonal antibody (dilution, 1:5000, Sigma-Aldrich Co., St Louis, MO) to control protein loading.

Immunohistochemical analysis. Immunohistochemistry was performed on Huh7 and HepG2 cells cultured on the slide glass in a six-well plate. After incubation, the cells were washed in PBS, fixed with 3% paraformaldehyde/2% sucrose/PBS for 10 min at room temperature, and permeabilized with 0.5% Triton X (Sigma-Aldrich Corporation, St. Louis, MO, USA). The fixed cells were incubated for 10 min at room temperature in PBS with 3% bovine serum albumin to avoid nonspecific binding. The detection of Ras and RhoA was carried out by incubation of the cells with polyclonal primary antibodies against Ras and RhoA for 1 h at room temperature. After washing, the cells were incubated with fluorescein-isothiocyanate (FITC)-conjugated mouse derived secondary antibody for 1 h at room temperature. The cell membrane was leveled with anti-EpCAM polyclonal antibody (dilution, 1:1000, Abcam, Cambridge, MA, USA). To observe the formation of stress fibers, we also performed immunohistochemistry with β-actin polyclonal antibody as described above.

Flow cytometric analysis. Hepatoma cells were incubated with 1, 10, or 100 μM of ZOL for 48 h. For the cell cycle assay, they were harvested and subjected to centrifugation, and 1×10^6 cells/mL were incubated in the fluorochrome solution. DNA content was determined by flow cytometry and the cell cycle phase distribution was analyzed with BrdU flow kit (BD PharMingen, Franklin Lakes, NJ, USA). Respective to their phase-specific DNA content, the cells were divided into G0/G1, S, and G2/M phases.

Terminal deoxynucleotidyl transferase-mediated dUTP-biotin nick-end labeling (TUNEL) assay analysis. The TUNEL method was performed to label 3′-end of fragmented DNA of apoptotic Huh7 and HepG2 cells. The apoptotic cells were stained by the TUNEL method, using an *in situ* cell death detection kit (Roche Diagnostics, Basel, Switzerland), according to the instructions provided by the manufacturer. The FITC-labeled TUNEL-positive cells were imaged under a fluorescent microscopy at 488-nm excitation and 530-nm emission wavelengths.

Caspase-3 activity assay. Caspase-3 inactivates inhibitor of caspase-activated deoxyrinonuclease and indirectly activates

caspase-activated deoxyrinonuclease, and it is related to chromatin fragmentation for nucleosome unit. We examined caspase-3 activity in ZOL-treated cells using Apopcyto Caspase-3 fluorometric Assay kit (Medical & Biological Laboratories, Nagoya, Japan).

Statistical analysis. Results are expressed as mean ± standard error of mean. Differences between experimental groups were analyzed by the *t*-test. Differences were considered significant when $P < 0.05$.

Results

ZOL inhibits proliferation of hepatoma cells. The effects of various concentrations of ZOL on the viability of Huh7 and HepG2 cells were studied after 48-h incubation using the cell viability assay. ZOL reduced the viability of both Huh7 and HepG2 cells in a dose-dependent manner (Fig. 1).

ZOL inhibits hepatoma cell migration. Next, we analyzed the effects of ZOL on the migration of hepatoma cells using the scratch assay. The width of the line scraped on the monolayer of Huh7 and HepG2 was measured under various concentrations of ZOL. Although ZOL had no effects on cell viability at the low concentrations (< 10 μM), the cell migration into the scraped line was suppressed at concentrations ≥ 10 μM. (Fig. 2)

ZOL inhibits cell proliferation and migration by preventing cytosol-to-cell membrane translocation of small G-proteins. As mentioned above, it is known that ZOL inhibits farnesyl pyrophosphate synthase, a key enzyme in the mevalonate pathway. First, we examined the effects of ZOL on the expression of RAS and RhoA, which are proteins located downstream of the mevalonate pathway. After incubation with ZOL at different concentrations for 24 h, proteins were extracted from the whole cell lysate and subjected to immunoblotting. The latter showed similar expression patterns for small G-protein in the control cells and cells treated with ZOL (data not shown).

Prenylation is the addition of hydrophobic molecules to facilitate the attachment of protein to the cell membranes. Prenylation of small G-proteins, such as Ras and RhoA, is considered an important process in protein–membrane interaction, which subsequently triggers cell proliferation and cell migration.[20–23] Therefore, we examined the effect of ZOL on the translocation of Ras and RhoA from the cytosol to the cell membrane of Huh7 and HepG2 cells. After 12-h cell incubation, Ras was observed in both the cytosol and cell membrane in the control and 10 μM ZOL groups, but only in the cytosol of 100-μM ZOL-treated cells. Similarly, RhoA was observed in both the cytosol and membrane under control conditions, but only in the cytosol in 10-μM ZOL-treated cells (Fig. 3). These findings suggest that ZOL inhibited prenylation of these small G-proteins. Thus, inhibition of prenylation of RhoA altered the formation of stress fibers and eventually changed the cell morphology (Fig. 3).

In order to prove that Ras inhibition by ZOL surely suppressed the cell viability, both cancer cells with Kras wild type and Kras mutant were treated with ZOL and then that cell viability was examined. Expectedly, the effectiveness of ZOL against Kras mutant cells was not as good as that against Kras wild cells. (Fig. S1)

ZOL inhibits Erk1/2 phosphorylation, pro-apoptotic protein overexpression, and promotes apoptosis of hepatoma cells. In the next series of experiments, we examined the effects of inhibition of G-protein prenylation. To this end, we examined mitogen-activated protein kinase (MAPK) pathway and apoptosis of hepatoma cells because they are associated with cell survival and cell death. ZOL inhibited Erk1/2 phosphorylation, which is phosphorylated downstream of Ras (Fig. 4a). This result suggests that ZOL causes downregulation of cell proliferation signals through the prevention of

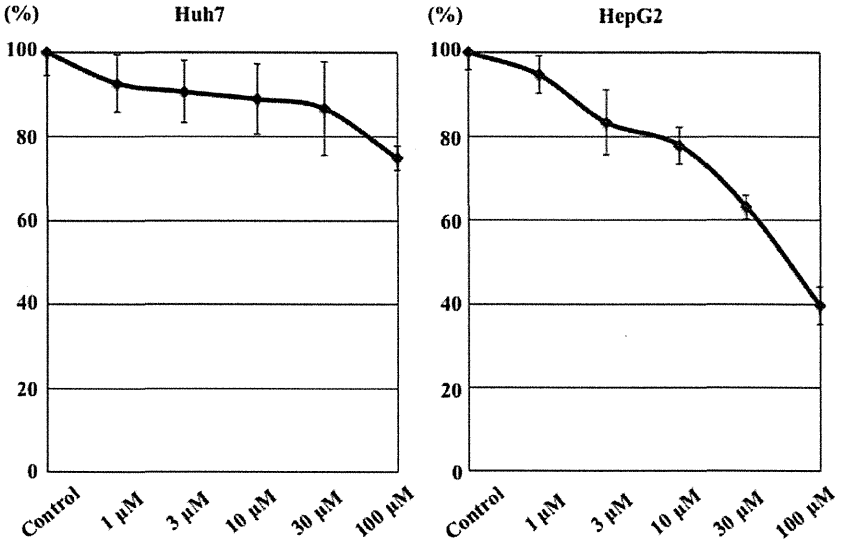

Figure 1 Zoledronic acid (ZOL) inhibits hepatoma cell growth in a dose-dependent manner. Huh7 and HepG2 cells were seeded at 1×10^4 per well and the cell number was counted after 48 h in the presence or absence of ZOL. Cell viability at each concentration of ZOL is indicated as percentage compared with that of hepatoma cells without ZOL. Data are mean ± SEM of six experiments.

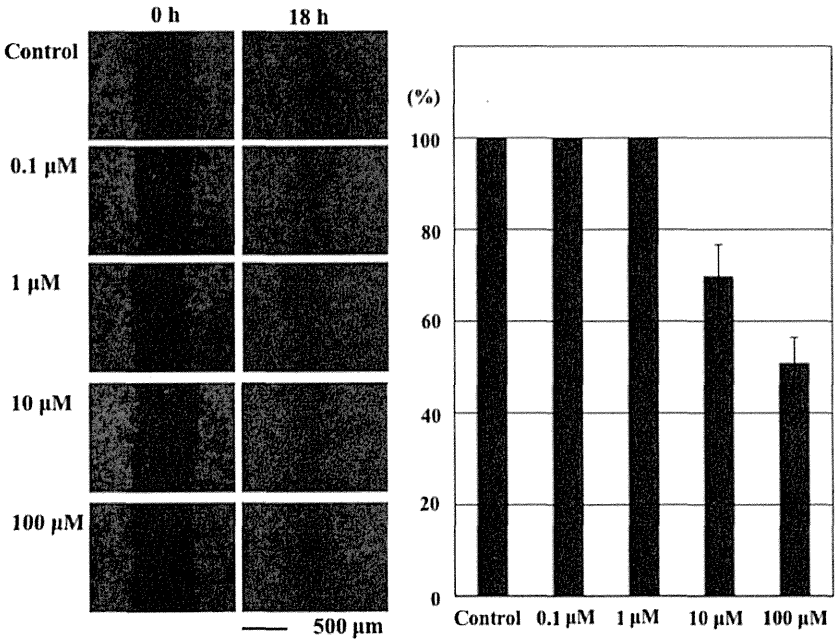

Figure 2 Effect of increasing concentrations of zoledronic acid (ZOL) on hepatoma cell migration through the scratched line. *Left:* The cell monolayer was scraped in a straight line using a p200 pipette tip, removed the debris, and added the indicated concentration of ZOL to the dishes. After 18-h incubation at 37°C, we compared the width of the scratched line before and after incubation. *Right:* The mean and standard deviation of the width of the scratch line was calculated for each concentration of ZOL in three experiments. Similar changes were noted in HepG2 cells (data not shown).

small G-protein prenylation. In another experiment, ZOL dose-dependently upregulated Bak and Bax in hepatoma cells (Fig. 4a), but had no effect on the expression of Mcl-1 and Bcl-xL. The intensity is as following: Bak (control:1.2 ± 0.2, 1 μM: 3.3 ± 0.2, 10 μM: 4.5 ± 0.7, 100 μM: 5.2 ± 0.7), Bax (control: 3.5 ± 0.5, 1 μM: 3.8 ± 0.6, 10 μM: 4.0 ± 0.7, 100 μM: 4.6 ± 0.7), Bcl-XL (control: 7.1 ± 0.9, 1 μM: 7.1 ± 1.0, 10 μM: 7.2 ± 1.3, 100 μM: 7.3 ± 1.2), Mcl-1 (control: 1.6 ± 0.5, 1 μM: 1.8 ± 0.5, 10 μM: 1.9 ± 0.5. 100 μM: 1.8 ± 0.5), β-actin (control: 4.6 ± 0.2, 1 μM: 4.6 ± 0.2, 10 μM 4.7 ± 0.1, 100 μM 4.7 ± 0.1). (Average ± standard deviation, intensity; $\times 10^{1}$)

We also investigated the effect of ZOL on the cell cycle phase distribution of hepatoma cells after 48-h treatment. The analysis demonstrated that approximately 74.0% of Huh7 cells were in G0/G1, 14.4% in G2/M, and 11.7% in the S phase (Fig. 4b). In contrast, ZOL dose-dependently increased the percentage of cells in the S phase.

Finally, we studied the effect of ZOL on apoptotic cell death. After 12-h incubation, few TUNEL-positive cells were noted among cells incubated with low concentration of ZOL (< 10 μM). However, the percentage of TUNEL-positive cells increased under high concentrations of ZOL (> 10 μM) (Fig. 5a). In other experiments, ZOL dose-dependently reduced caspase-3 activity in both Huh7 cells after 12-h incubation (Fig. 5b).

Discussion

Radiotherapy[24] and percutaneous cementoplasty[25] are currently being used for the treatment of bone metastasis from HCC, based on alleviation of pain and inhibition of tumor progression. However, the effects of both treatments are locoregional; therefore, it is difficult to select these treatment for multiple bone metastases. On the other hand, ZOL is a systemically administered drug and is considered the antitumor agent for multiple metastatic lesions.

Since the introduction of ZOL into clinical use for bone metastasis of solitary tumors in Japan, its benefits have been described in breast and prostate cancers, which tend to metastasize to bones. ZOL is also effective against HCC, and our group was among the first to report the clinical effects of ZOL against bone metastasis of HCC.[10] Our retrospective cohort study investigated the efficacy of ZOL against bone metastases and reported that ZOL delayed both pain progression and radiographic progression of bone metastases, probably through prevention of migration of HCC into surrounding tissues. Accordingly, the present study analyzed the mechanism of the antitumor effect of ZOL on HCC study.

In the present study, we first analyzed the effects of ZOL on hepatoma cells. After 48-h incubation at 37°C, ZOL dose-dependently reduced cell viability. Further analysis showed that ZOL has potent anti-invasive properties, preventing the migration of these cells. These findings suggested that ZOL modulates both cell growth and cell migration. Analysis of the anti-proliferative and anti-invasive effects of ZOL showed inhibition of farnesyl pyrophosphate synthase, a key enzyme in the mevalonate pathway, with subsequent inhibition of prenylation of small G-proteins.[17,18] Moreover, as a supplemental data, we confirmed that ZOL was not effective against Kras mutant cells, in which Kras has been activated spontaneously.

Next, we used immunohistochemistry to determine the effects of ZOL on the translocation of small G-proteins cell from the cytoplasm to membrane and the effect of the latter on cell proliferation and migration. The results showed dyslocation of small G-protein after treatment with ZOL. These findings indicate the importance of small G-protein translocation in the activation of

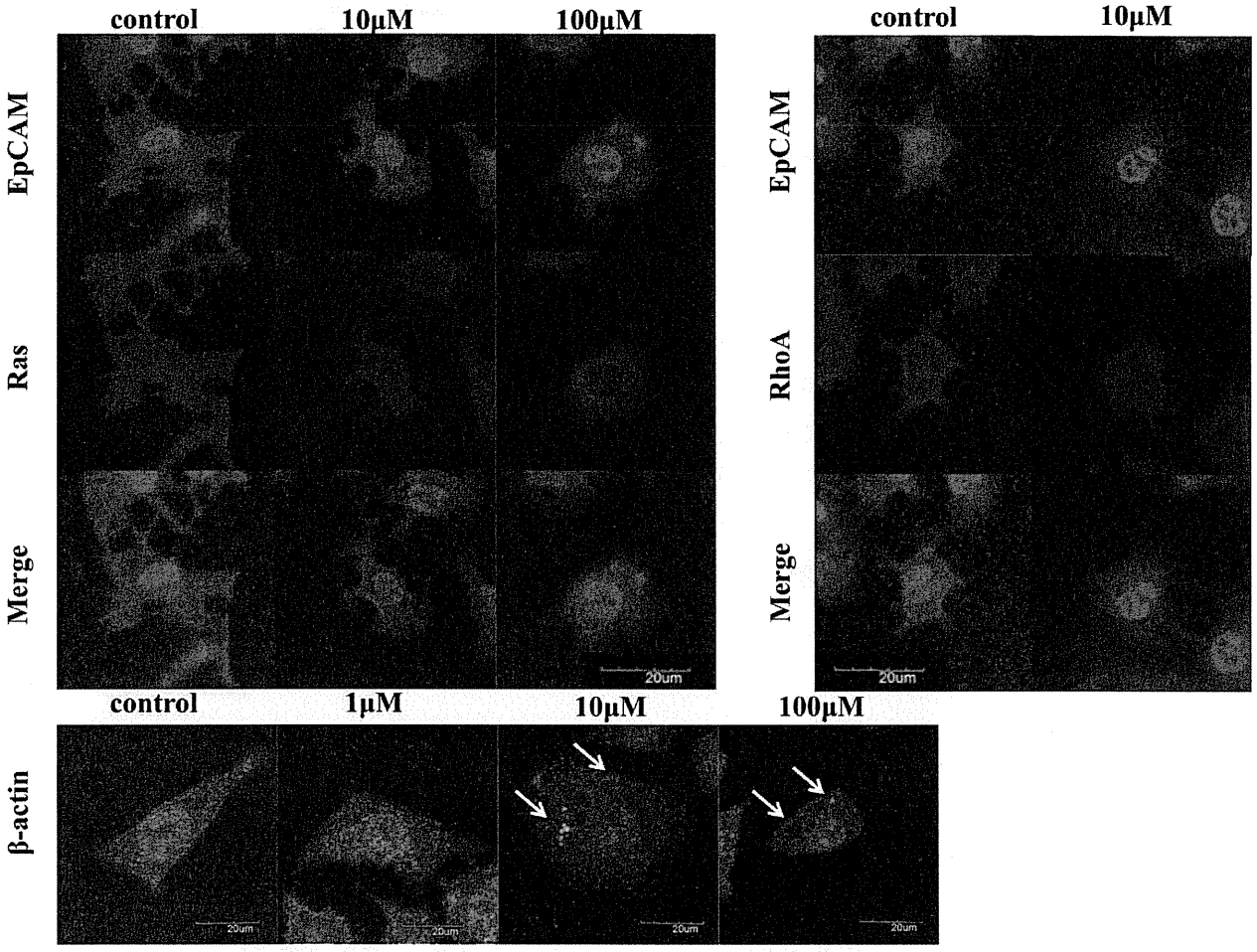

Figure 3 Translocalization of Ras and RhoA under zoledronic acid (ZOL) treatment. Huh7 cells were treated with or without ZOL for 12 h. *Top:* The location of Ras and RhoA was analyzed by confocal microscopy. The cell membrane was labeled with anti-EpCAM antibody. *Bottom:* The stress fiber was labeled with anti-β-actin antibody. Abnormal stress fibers could be seen as green dots pointed with white arrow. Scale bar 20 μm. Similar changes were noted in HepG2 cells (data not shown).

MAPK pathway and that ZOL can prevent such translocation. In this regard, Danoyelle *et al.*[26] reported similar results in MDA-MB-231 cells.

The antiproliferative effect of ZOL correlated also with changes in cell cycle distribution as indicated by the accumulation and arrest of tumor cells in the S phase. This observation is in agreement with the results of previous studies that examined the same effects on different types of tumor cells, which suggested arrest of ZOL-treated cells in the S phase.[27–31]

We also examined the role of ZOL on apoptosis. The Bcl-2 family proteins regulate the release of cytochrome c into the cytosol and control the activation of caspases and the apoptotic process. Bak and Bax are pro-apoptotic members of the Bcl-2 family, serve to release cytochrome c from the mitochondria, and initiate the caspase activation pathway for apoptosis. On the other hand, Mcl-1 and Bcl-xL antagonize the actions of pro-apoptotic Bcl-2 family members and inhibit apoptosis. The ratio of anti-apoptotic members to pro-apoptotic members might influence cell susceptibility to apoptosis. Our results showed exposure to ZOL, activated the expression of pro-apoptotic proteins, decreased the anti-apoptotic proteins/pro-apoptotic proteins ratio, and promoted apoptosis, in hepatoma cells.

The present study on HCC and previous studies on breast cancer and prostate cancer,[26,32] highlighted the antitumor property of ZOL, which is based on inhibiting mevalonate pathway. This effect could be elicited not only on metastatic lesions, but also on primary tumors, and should improve prognosis. Aft *et al*[33] reported recently better prognosis of breast cancer patients treated with ZOL compared with those without. Similarly, we reported previously that treatment with ZOL tends to improve prognosis of HCC patients with bone metastasis compared with non-ZOL-based treatment.[10] These clinical outcomes support our finding that ZOL affects both metastatic bone tumor and primary tumor. These data prompt us to apply the combination therapies, such as ZOL plus radiotherapy or ZOL plus cementplasty, for systemic HCC metastases.

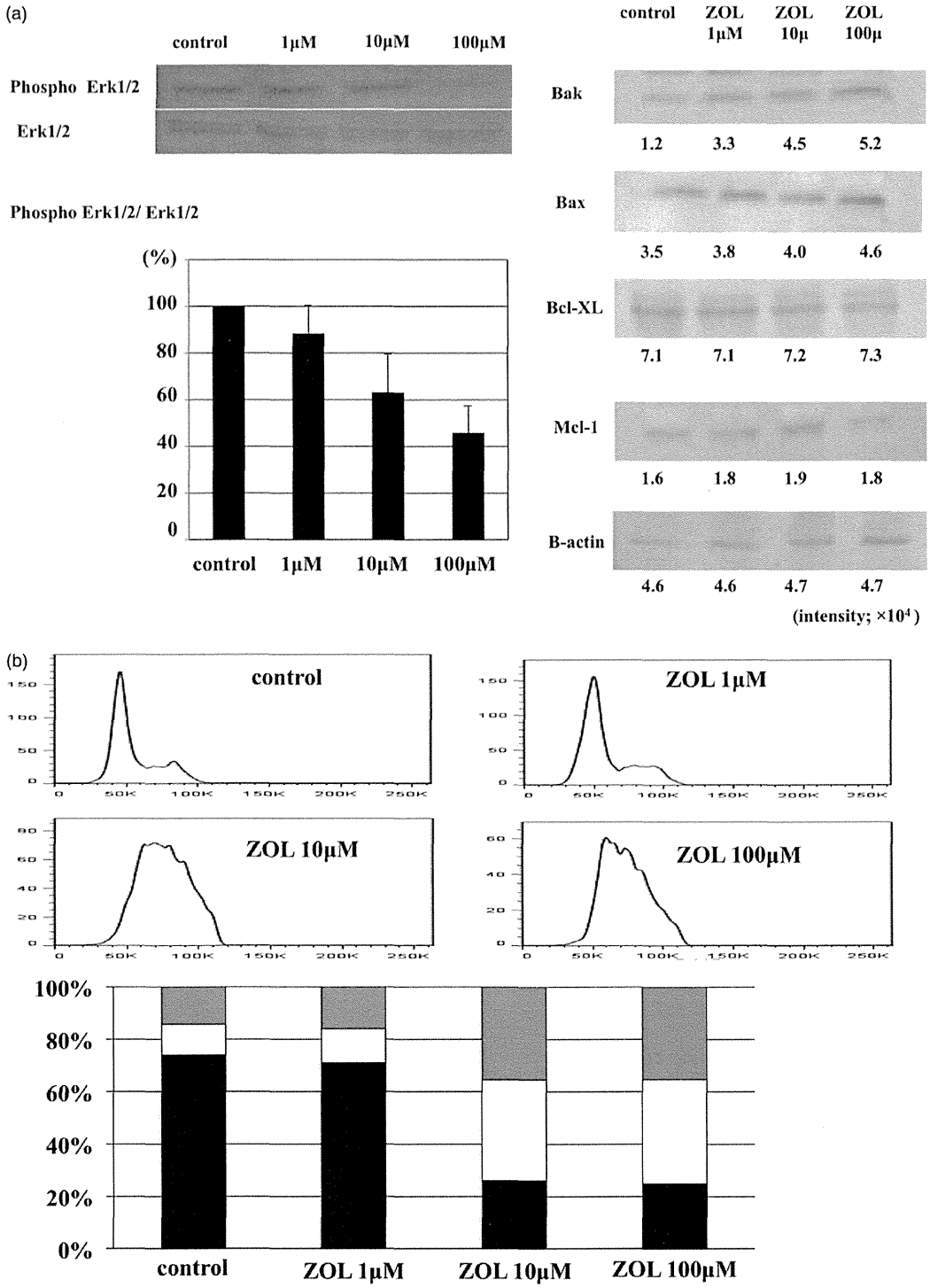

Figure 4 Phosphorylation of Erk1/2. (a) *Left:* In mitogen-activated protein kinase cascade, downstream of Ras, zoledronic acid (ZOL) inhibited Erk1/2 phosphorylation. *Right:* Expression of anti-apoptotic proteins/pro-apoptotic proteins. Note the dose-dependent upregulation of Bak and Bax in hepatoma cells. The numbers below indicate the signal intensity. Equal amounts of protein were loaded. β-actin was used as a positive control. (b) *Top:* Results of flow cytometric analysis of DNA content in Huh7 cells, in the absence or presence of 1, 10, or 100 μM of ZOL for 48 h. *Bottom:* Percentage of cells at each cycle phase. Replicate experiments yielded similar results. Similar changes were noted in HepG2 cells (data not shown). ▩, G0/G1; □, S; ▩, G2/M.

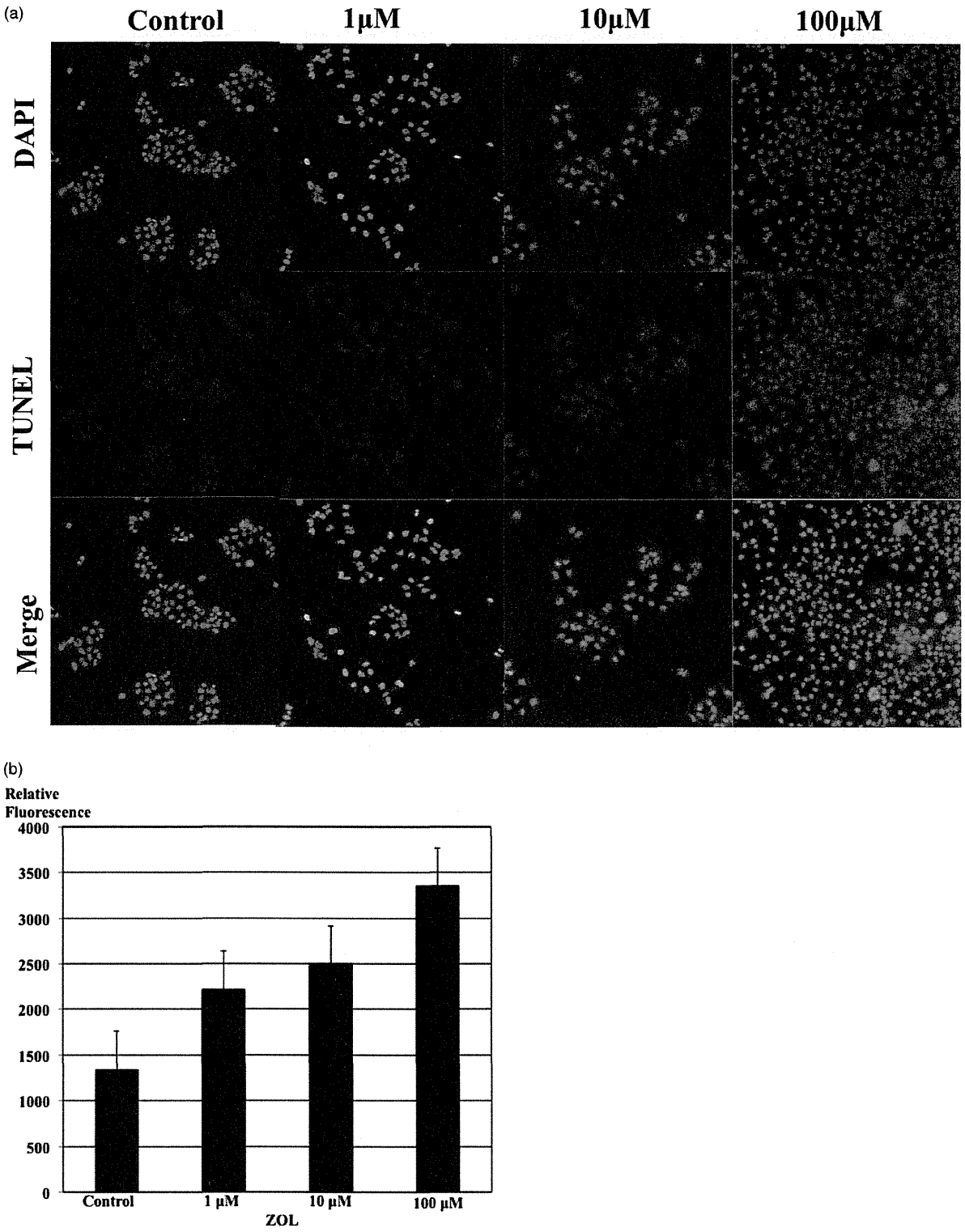

Figure 5 Zoledronic acid (ZOL) induces apoptosis of hepatoma cells. (a) Confluent Huh7 cells were incubated for 12 h with ZOL at the indicated concentration. Images of terminal deoxynucleotidyl transferase-mediated dUTP-biotin nick-end labeling (TUNEL)-positive cells were captured by a fluorescence microscope (200 ×). (b) ZOL dose-dependently reduced caspase-3 activity in Huh7 cells. Similar changes were noted in HepG2 cells (data not shown). DAPI, 4′,6-diamidino-2-phenylindole.

The present study has certain limitations. Although we confirmed the antitumor effect of ZOL, this effect was not tested using tumor tissue but by using tumor cell lines. It is uncertain whether the same antitumor effect and mechanism of action would be observed *in vivo*. Furthermore, there are data available on blood ZOL concentrations that are achieved during treatment of cancer patients. Although ZOL is usually taken up by osseous tissue and the remainder is excreted by the kidney within few hours, ZOL's optimal dose need to be determined for each type of cancer, for both primary cancer and metastasis. Nevertheless, our data highlight the promising potential of ZOL in the treatment of bone metastasis from HCC.

Conclusion. Our *in vitro* study demonstrated that ZOL prevented cell growth and migration based on direct antitumor effect in HCC cell lines. The clinical use of ZOL could not only improve local control of bone metastasis, but also prevent growth of primary lesion and new metastatic lesions of HCC. Further studies, including improvement of ZOL drug delivery or its use in combination with other chemotherapeutic agents, might help improve the prognosis of HCC patients with bone metastasis.

Acknowledgment

Data analysis of this study was carried out in cooperation with the analysis center of Life Science, Natural Science Center for Basic Research and Development, Hiroshima University.

References

1 Nakano M, Ando E, Sato M *et al.* Recent progress in the management of hepatocellular carcinoma detected during a surveillance program in Japan. *Hepatol. Res.* 2010; **40**: 989–96.
2 Arii S, Sata M, Kudo M *et al.* Management of hepatocellular carcinoma: report of Consensus Meeting in the 45th Annual Meeting of the Japan Society of Hepatology (2009). *Hepatol. Res.* 2010; **40**: 667–85.
3 Okita K. Management of hepatocellular carcinoma in Japan. *J. Gastroenterol.* 2006; **41**: 100–6.
4 Uka K, Aikata H, Chayama K *et al.* Pretreatment predictor of response, time to progression, and survival to intraarterial 5-fluorouracil/interferon combination therapy in patients with advanced hepatocellular carcinoma. *J. Gastroenterol.* 2007; **42**: 845–53.
5 Kamada K, Kitamoto M, Aikata H *et al.* Combination of transcatheter arterial chemoembolozation using cisplatin-lipiodol suspension and percutaneous ethanol injection for treatment of advanced small hepatocellular carcinoma. *Am. J. Surg.* 2002; **184**: 284–90.
6 Rossi S, Di Stasi M, Buscarini E *et al.* Percutaneous RF interstitial thermal ablation in the treatment of hepatic cancer. *ALR. Am. J. Roentgenol.* 1996; **167**: 759–68.
7 Uka K, Aikata H, Takaki S *et al.* Clinical features and prognosis of patients with extrahepatic metastases from hepatocellular carcinoma. *World J. Gastroenterol.* 2007; **13**: 414–20.
8 Natsuizaka M, Omura T, Akaike T *et al.* Clinical features of hepatocellular carcinoma with extrahepatic metastases. *J. Gastroenterol. Hepatol.* 2005; **20**: 1782–7.
9 Katyal S, Oliver JH III, Peterson MS, Ferris JV, Carr BS, Baron RL. Extrahepatic metastases from hepatocellular carcinoma. *Radiology* 2000; **216**: 698–703.
10 Katamura Y, Aikata H, Cyayama K *et al.* Zoledronic acid delays disease progression of bone metastases from hepatocellular carcinoma. *Hepatol. Res.* 2010; **2010**: 1195–203.
11 Boissier S, Magnetto S, Frappart L *et al.* Bisphosphonates inhibit prostate and breast carcinoma cell adhesion to unmineralized and mineralized bone extracellular matrices. *Cancer Res.* 1997; **57**: 3890–4.
12 Boissier S, Ferreras M, Peyruchaud O *et al.* Bisphosphonates inhibit breast and prostate carcinoma cell invasion, an early event in the formation of bone metastases. *Cancer Res.* 2000; **60**: 2949–54.
13 Fromigue O, Lagneaux L, Body JJ. Bisphosphonates induce breast cancer cell death in vitro. *J. Bone Miner. Res.* 2000; **15**: 2211–21.
14 Senaratne SG, Pirianov G, Mansi JL *et al.* Bisphosphonates induce apoptosis in human breast cancer cell lines. *Br. J. Cancer* 2000; **82**: 1459–68.
15 Hiraga T, Williams PJ, Mundy GR *et al.* The bisphosphonate ibandronate promotes apoptosis in MDA-MB-231 human breast cancer cells in bone metastases. *Cancer Res.* 2001; **61**: 4418–24.
16 Jagdev SP, Coleman RE, Shipman CM *et al.* The bisphosphonate, zoledronic acid, induces apoptosis of breast cancer cells: evidence for synergy with paclitaxel. *Br. J. Cancer* 2001; **84**: 1126–34.
17 Hosfield DJ, Zhang Y, Dougan DR *et al.* Structural basis for bisphosphonate-mediated inhibition of isoprenoid biosynthesis. *J. Biol. Chem.* 2004; **5**: 8526–9.
18 Dunford JE, Thompson K, Coxon FP *et al.* Structure-activity relationships for inhibition of farnesyl diphosphate synthase in vitro and inhibition of bone resorption in vivo by nitrogen-containing bisphosphonates. *J. Pharmacol. Exp. Ther.* 2001; **296**: 235–42.
19 Liang CC, Park AY, Guan JL. In vitro scratch assay: a convenient and inexpensive method for analysis of cell migration in vitro. *Nat. Protoc.* 2007; **2**: 329–33.
20 Santini D, Caraglia M, Vincenzi B *et al.* Mechanisms of disease: preclinical reports of antineoplastic synergistic action of bisphosphonates. *Nat. Clin. Pract. Oncol.* 2006; **3**: 325–38.
21 Yoshioka K, Matsumura F, Akedo H *et al.* Small GTP-binding protein Rho stimulates the actomyosin system, leading to invasion of tumor cells. *J. Biol. Chem.* 1998; **273**: 5146–54.
22 Kuroda J, Kimura S, Segawa H *et al.* The third-generation bisphosphonate zoledronate synergistically augments the anti-Ph+ leukemia activity of imatinib mesylate. *Blood* 2003; **15**: 2229–35.
23 Kimura S, Kuroda J, Segawa H *et al.* Antiproliferative efficacy of the third-generation bisphosphonate, zoledronic acid, combined with other anticancer drugs in leukemic cell lines. *Int. J. Haematol.* 2004; **79**: 37–43.
24 Seong J, Koom WS, Park HC *et al.* Radiotherapy for painful bone metastases from hepatocellular carcinoma. *Liver Int.* 2005; **25**: 261–5.
25 Kodama H, Aikata H, Chayama K *et al.* Efficacy of percutaneous cementoplasty for bone metastasis from hepatocellular carcinoma. *Oncology* 2007; **72**: 285–92.
26 Danoyelle C, Hong L, Soria C *et al.* New insights into the actions of bisphosphonate zoledronic acid in breast cancer cells by dual RhoA-dependent and -independent effects. *Br. J. Cancer* 2003; **88**: 1631–40.
27 Coleman RE. Skeletal complications of malignancy. *Cancer* 1997; **80** (Suppl. 8): 1588–94.
28 Bloomfield DJ. Should bisphosphonates be part of the standard therapy of patients with multiple myeloma or bone metastases from other cancers? An evidence-based review. *J. Clin. Oncol.* 1998; **16**: 1218–25.
29 Rosen LS, Gordon D, Tchekmedyian S *et al.* Zoledronic acid versus placebo in the treatment of skeletal metastases in patients with lung cancer and other solid tumors: a phase III, double-blind, randomized

trial-the Zoledronic Acid Lung Cancer and Other Solid Tumors Study Group. *J. Clin. Oncol.* 2003; **21**: 3150–7.
30 Caraglia M, D'Alessandro AM, Marra M *et al.* The farnesyl transferase inhibitor R115777 (Zarnestra) synergistically enhances growth inhibition and apoptosis induced on epidermoid cancer cells by zoledronic acid (Zometa) and pamidronate. *Oncogene* 2004; **23**: 6900–13.
31 Yeh KY, McAdam AJ, Pulaski BA, Shastri N, Frelinger JG, Lord EM. IL-3 enhances both presentation of exogenous particulate antigen in association with class I major histocompatibility antigen and generation of primary tumor-specific cytolytic T lymphocytes. *J. Immunol.* 1998; **160**: 5773–80.
32 Neville-Webbe HL, Rostami-Hogjegan A, Holen I *et al.* Sequence- and schedule-dependent enhancement of zoledronic acid induced apoptosis by doxorubicin in breast and prostate cancer cells. *Int. J. Cancer* 2005; **20**: 364–71.
33 Aft RL, Naughton M, Weilbaecher K *et al.* Effect of (Neo) adjuvant zoledronic acid on disease-free and overall survival in clinical stage II/III breast cancer. *Br. J. Cancer* 2012; **107**: 7–11.

Supporting information

Additional Supporting Information may be found in the online version of this article at the publisher's web-site:

Method S1 Cell proliferation. For the proliferation assay, we used the concentration of FBS (10%) to allow sufficient viability of WiDr (colon cancer cells with Kras wild type) and DLD1 (colon cancer cells with Kras mutant) cells. Just after trypsinization, the cells were seeded at a concentration of 1×10^4 cells per well in a 96-well plate and incubated with ZOL for 24 h. Cell viability was measured 48 h later for WiDr and DLD1 cells using the Cell Quanti-Blue Cell Viability Assay Kit (Bio Assay Systems, USA).

Method S2 Cell proliferation. For the proliferation assay, we used the concentration of FBS (10%) to allow sufficient viability of Huh7 and HepG2 cells. Just after trypsinization, the cells were seeded at a concentration of 1×10^4 cells per well in a 96-well plate and incubated with ZOL for 24 h. Cell viability was measured 48 h later for Huh7 and HepG2 cells using the Cell Quanti-Blue Cell Viability Assay Kit (Bio Assay Systems, USA).

Figure S1 Zoledronic acid inhibits the cell growth of Kras wild-type cells, but not Kras mutant cells. WiDr (colon cancer cells with Kras wild type) and DLD1 (colon cancer cells with Kras mutant) cells were seeded at 1×10^4 per well and the cell number was counted after 12, 24, 36, and 48 h in the presence or absence of ZOL. Cell viability at each concentration of ZOL is indicated as percentage compared to that of colon cancer cells without ZOL. Data are mean ± SEM of six experiments.

Figure S2 Zoledronic acid inhibits hepatoma cell growth in a dose- and time-dependent manner. Huh7 and HepG2 cells were seeded at 1×10^4 per well and the cell number was counted after 12, 24, 36, and 48 h in the presence or absence of ZOL. Cell viability at each concentration of ZOL is indicated as percentage compared with that of hepatoma cells without ZOL. Data are mean ± SEM of six experiments.

JOURNAL OF VIRAL HEPATITIS
JVH

Journal of Viral Hepatitis, 2015, 22, 166–174 doi:10.1111/jvh.12275

Ribavirin dose reduction during telaprevir/ribavirin/peg-interferon therapy overcomes the effect of the ITPA gene polymorphism

S. Akamatsu,[1,2,3,*] C. N. Hayes,[1,2,*] M. Tsuge,[1,2,4] E. Murakami,[1,2] N. Hiraga,[1,2] H. Abe,[1,2] D. Miki,[1,2,3] M. Imamura,[1,2] H. Ochi[1,2,3] and K. Chayama[1,2,3] Hiroshima Liver Study Group

[1]*Department of Gastroenterology and Metabolism, Applied Life Sciences, Institute of Biomedical & Health Sciences, Hiroshima, Japan;* [2]*Liver Research Project Center, Hiroshima University, Hiroshima, Japan;* [3]*Laboratory for Digestive Diseases, SNP Research Center, The Institute of Physical and Chemical Research (RIKEN), Hiroshima, Japan; and* [4]*Natural Science Center for Basic Research and Development, Hiroshima University, Hiroshima, Japan*

Received January 2014; accepted for publication May 2014

SUMMARY. Treatment success of chronic hepatitis C virus genotype 1 infection has improved with the advent of telaprevir plus peg-interferon/ribavirin triple combination therapy. However, the effect of inosine triphosphatase (ITPA) polymorphism on dose reduction during triple therapy, especially during the postmarketing phase, has not been sufficiently evaluated. We analysed 273 patients with genotype 1 infection who were treated with triple therapy and assessed the effect of the ITPA polymorphism on dose reduction. ITPA and IFNL4 SNP genotypes were determined by the Invader assay. A stepwise multivariate regression analysis was performed to identify factors associated with outcome of the therapy. The overall sustained viral response (SVR) rate 12 weeks after the end of therapy was 80.2% (219/273). Decline of haemoglobin was significantly faster, and ribavirin was more extensively reduced in patients with ITPA SNP rs1127354 genotype CC than CA/AA. Extensive reduction of ribavirin resulted in mild reduction of telaprevir and peg-interferon, but no significant increase in viral breakthrough. Although the amount of telaprevir given was slightly higher in CA/AA patients, the total dose of peg-interferon and the SVR rate did not differ between the two groups. Multivariate analysis showed that IFNL4 but not ITPA SNP genotype, platelet count and peg-interferon adherence were significantly associated with outcome of therapy. Postmarketing-phase triple therapy resulted in a high SVR rate in spite of extensive ribavirin dose reduction in a diverse patient population, indicating the importance of treatment continuation and appropriate management of adverse events.

Keywords: anaemia, dose reduction, haemoglobin, hepatitis C virus, sustained viral response.

Hepatitis C virus (HCV) infection is a serious global health problem affecting more than 200 million people [1]. With the introduction of protease inhibitors, the sustained viral response (SVR) rate with peg-interferon, ribavirin and telaprevir/boceprevir triple therapy has improved from 50% to 70% for genotype 1 [2]. While response to therapy varies depending upon prior treatment history, increases in each group have been observed, including up to 92% in treatment-naive patients [3], 86% in prior relapsers, 57% in prior partial responders and 31% in prior null responders [2,4].

Although the eradication rate has improved substantially, a number of issues remain, including premature termination due to anaemia [5–8], skin rash [6,9–11] and renal damage [12–14]. However, some potentially difficult-to-treat patients might respond successfully to triple therapy. For example, patients with advanced fibrosis were successfully treated with a relatively high eradication rate [15], although in other studies, the safety profile was poor, and patients with a platelet count ≤100 000/mm [12] and serum albumin <35 g/L should not be treated with triple therapy [7].

A fixed, three times daily 750 mg telaprevir dose without reduction or interruption is recommended [16]. However, the recommended dose was determined based on

Abbreviations: HCV, Hepatitis C virus; ITPA, inosine triphosphatase; SVR, sustained viral response.

Correspondence: Kazuaki Chayama, Department of Gastroenterology and Metabolism, Applied Life Sciences, Institute of Biomedical and Health Sciences, Hiroshima University, 1-2-3 Kasumi, Minami-ku, Hiroshima-shi, Hiroshima 734-8551, Japan.
E-mail: chayama@hiroshima-u.ac.jp
*Authors contributed equally.

studies conducted in the USA and Europe [17], whereas Japanese participants in telaprevir clinical trials tended to have body weights 15–30 kg lower than their American and European counterparts, resulting in severe side effects at this dosage [18]. To avoid treatment discontinuation, Suzuki *et al.* [19] reduced the dose of telaprevir from 2250 mg/day to 1500 mg/day and did not observe a worsening of the sustained viral response (SVR) rate. We also compared 2250 mg and 1500 mg telaprevir doses in a randomized clinical trial and showed that telaprevir discontinuation was significantly reduced with the smaller dose even though the SVR rate (92%) and viral dynamics did not differ significantly during treatment [20]. Therefore, mild telaprevir dose reduction might help to avoid strong side effects without compromising the SVR rate in patients with lower body weight.

Ribavirin was reduced extensively in the above studies to avoid premature termination, but ribavirin remains necessary to prevent viral breakthrough, so a safe balance must be determined. Several single-nucleotide polymorphisms in the inosine triphosphatase (ITPA) locus (rs7270101 and rs1127354) have been reported to influence the incidence of anaemia [7,15,21–24]. While the rs7270101 A allele is fixed in Asian populations (HapMap JPT, HCB = 1.000), Japanese patients with the rs1127354 CC genotype are prone to developing severe anaemia during therapy [22,23]. In this study, we assessed the influence of ITPA polymorphism only in patients who began triple therapy after telaprevir was approved. This restriction is important because pre-approval clinical trials included mainly younger and nonanaemic patients, but patients in Japan tend to be on average 10 years older than in western countries and include a higher proportion of women, for whom ribavirin-induced anaemia is of particular concern [25]. Findings from this study may apply to other countries with older patients awaiting a safer treatment regimen.

METHODS

Patients

From December 2011 to May 2013, 273 patients with chronic genotype 1 infection who were HCV RNA positive for more than 6 months with an HCV RNA titre higher than 5 log copy mL-1, as determined by the Roche HCV Amplicor assay, were enrolled in the study. Patients positive for active hepatitis B virus or human immunodeficiency virus infection markers were excluded. Basic characteristics of the patients are shown in Table 1. All patients provided written informed consent. The experimental protocol met the ethical guidelines of the World Medical Association Declaration of Helsinki and was approved by the Hiroshima University Ethical Committee.

Therapeutic regimen and evaluation of the therapy

Peg-interferon alpha 2b (Peg-Intron, MSD, Tokyo, Japan) and ribavirin (Rebetol, MSD, Tokyo, Japan) were administered according to patient body weight for 24 weeks, as described previously [18]. Telaprevir (Telavic, MSD, Tokyo, Japan) was given three times daily at an initial dose of 750 mg or 500 mg based on sex and baseline haemoglobin levels, and all drugs were reduced as necessary in accordance with dose reduction guidelines [18]. Briefly, for female patients with baseline haemoglobin levels <14 g/dL or male patients with baseline haemoglobin levels <13 g/dL, ribavirin dosage was reduced by 200 mg and telaprevir dosage were reduced to 1500 mg. Haemoglobin levels were closely monitored, and in the case of anaemia, ribavirin dosage was reduced based on both the absolute value of the haemoglobin levels as well as the amount of haemoglobin reduction. Patients who remained HCV RNA negative 12 weeks after the end of treatment were considered to have achieved SVR.

SNP genotyping

SNP genotyping for interferon lambda 4 (rs8099917 and ss469415590) and ITPA (rs1127354) was determined by the Invader assay as described previously [22].

Statistical analysis

Statistical analysis was performed using the R statistical package version 3.0.2 and SPSS statistics 19.0 (IBM SPSS Inc., Chicago, IL, USA). Continuous variables are reported using the median and range and were analysed using the nonparametric Mann–Whitney U-test. Count data was analysed using the chi-square test. Multivariate logistic regression was performed to identify factors associated with SVR using forward stepwise variable selection. Kaplan–Meier analyses were performed to estimate the cumulative incidence of dose reduction for ribavirin, telaprevir and peg-interferon.

RESULTS

Patients ranged in age from 24 to 79, and 49.5% were female (Table 1). Of the 273 patients who underwent triple therapy, 219 (80.2%) achieved SVR, 4.8% relapsed during follow-up, 5.5% experienced viral breakthrough during treatment, and 9.5% failed to respond to the therapy. A total of 61.1% of patients with fibrosis ≥3 achieved SVR, and 69.7% of patients with fibrosis ≥2 achieved SVR. Only 26% of patients were treatment-naive, but 78% of these patients achieved SVR. Among patients who had previously undergone interferon therapy, 79 (41.4%) were non-responders and 110 (57.6%) relapsed under prior therapy. A total of 90.1% of treatment-experienced patients

Table 1 Baseline patient characteristics

	Total (n = 273)	SVR (219)	non-SVR (54)
Sex (M/F)	138/135	110/109	28/26
Age	62 (24–79)	61 (24–79)	63 (27–79)
Body height (cm)	160 (134.5–181)	160.5 (134.5–181)	158.5 (142.7–179.5)
Body weight (kg)	60 (36.3–100.1)	60 (36.3–100.1)	60.4 (43–81.3)
HCV genotype (1b/1a/ND)	243/1/29	192/1/26	51/0/3
IL28B (TT/TG/GG/ ND)	165/78/3/27	152/40/0/27	13/38/3/0
ITPA (CC/CA/AA/ ND)	185/59/2/27	144/46/2/27	41/13/0/0
IFNλ4(TT/TT,TT/⊿G,⊿G/⊿G,ND)	146/77/3/47	136/40/0/43	10/37/3/4
HCV core70 (wild/mix/mutant/ND)	81/5/64/123	73/4/39/103	8/1/25/20
WBC ($10^3/\mu$L)	4890 (2400–11830)	4880 (2400–11830)	4900 (2400–7804)
Plt ($10^4/\mu$L)	16.3 (5.2–40.4)	16.8 (5.2–40.4)	12.4 (5.4–24.8)
Hb (g/dL)	13.9 (10–18.1)	14 (10–18.1)	13.5 (10.8–17)
AST (IU/L)	38 (5–200)	36 (5–200)	45 (16–145)
ALT (IU/L)	38 (10–286)	37 (10–286)	41 (13–204)
γGTP (IU/L)	31 (1–669)	30 (1–669)	43 (11–442)
HCV RNA (Log IU/mL)	6.6 (0–7.8)	6.6 (0–7.8)	6.6 (5–7.5)

ND, not determined. Continuous values are reported as median (range).

achieved SVR. A total of 53% of the prior nonresponders achieved SVR under triple therapy, whereas 95% of the prior relapsers achieved SVR. While 12 (15%) prior nonresponders experienced viral breakthrough during telaprevir treatment, only 1 (0.9%) prior relapser experienced viral breakthrough. Substitution at core amino acid 70 (core70) of the HCV core protein was strongly associated with viral breakthrough (P = 2.6E-17), and no viral breakthrough occurred in patients with wild-type core70. Viral breakthrough was also associated with baseline platelet count and adherence to telaprevir, peg-interferon and ribavirin in univariate analysis, although only IFNL4 genotype was significant (P = 0.028) when all factors were considered simultaneously.

Haemoglobin decline during triple therapy by ITPA SNP genotype and reduction of drugs

Patients with the anaemia-prone ITPA rs1127354 CC genotype showed a significantly more rapid decline in haemoglobin levels compared to patients with CA or AA genotypes (Fig. 1). Haemoglobin levels were significantly lower in CC patients than CA/AA patients at each time point for the first 4 weeks of therapy (Fig. 1). In response to haemoglobin decline, ribavirin, telaprevir and peg-interferon dosages were reduced as necessary according to treatment guidelines. The period without reduction of ribavirin was significantly shorter in patients with the rs1127354 CC genotype compared to CT/TT patients (P = 0.028; Fig. 2).

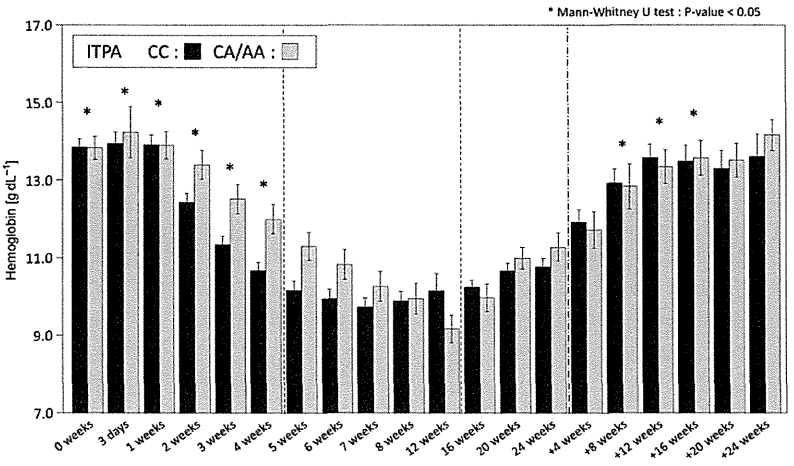

Fig. 1 Haemoglobin levels by ITPA rs1127354 genotype during 24 weeks of therapy and 24 weeks of follow-up. Dashed lines indicate treatment at 4 weeks, 8 weeks and end of treatment at 24 weeks.

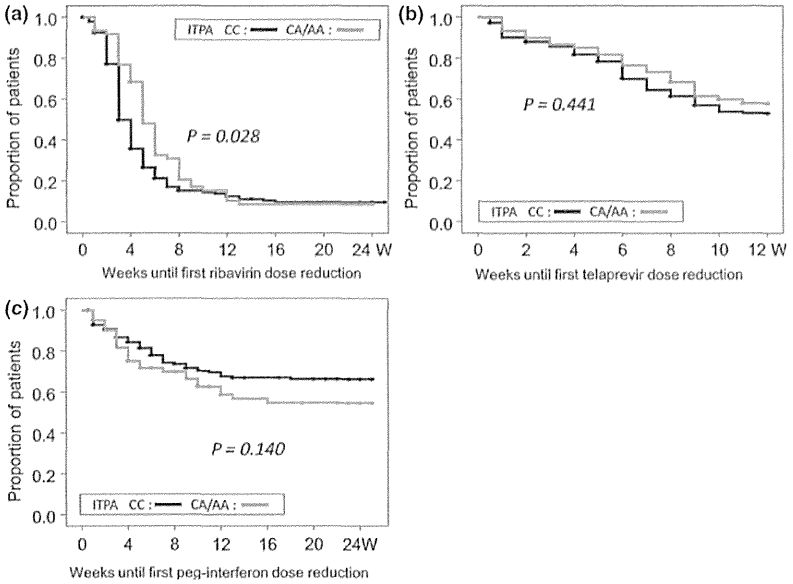

Fig. 2 Time until dose reduction by ITPA rs1127354 genotype. The difference in the number of weeks until the first dose reduction in rs1127354 CC *vs* CA/AA patients was determined by the log-rank test for (**a**) ribavirin, (**b**) telaprevir and (**c**) peg-interferon.

In contrast, the period without reduction for telaprevir ($P = 0.441$) and peg-interferon (0.140) was not significantly different among these patients, although it tended to be shorter in rs1127354 CC patients (Fig. 2). Consequently, the total amount of ribavirin given to each patient was significantly lower in rs1127354 CC patients (51470 mg) compared with CA/AA patients (63950 mg) ($P = 0.016$; Fig. 3). The difference in total amount of telaprevir given was less pronounced in CC (122030 mg) *vs* CA/AA (136170 mg) patients, but the difference was still statistically significant ($P = 0.024$), whereas there was no significant difference in total peg-interferon dosage (CC: 1699 mg *vs* CA/AA: 1781 mg; $P = 0.61$).

Effect of ITPA SNP genotype on total dosage of the drugs and outcome of therapy

Patients who achieved SVR received a significantly greater total amount of each of the three drugs (Fig. 3). However, when we assessed the effect of ITPA genotype on outcome of therapy, the SVR ratio between rs1127354 CC and CA/AA patients was not significantly different (144/185 [77.8%] *vs* 48/61[78.7%]; $P = 0.889$; Table 2). Among prior relapsers, 93% of CC patients and all CA/AA patients achieved SVR, whereas among prior nonresponders, 54% of CC patients and 44% of CA/AA patients achieved SVR.

Effect of adherence and duration of each drug on outcome of therapy

We further assessed the effect of adherence of each drug (defined as the amount of drug taken relative to the amount planned for each patient) with respect to outcome of therapy (Figure S1). All of the patients who received at least 90% of the planned dose of ribavirin achieved SVR, although the number of such patients was quite small ($n = 18$) and included 7 prior relapsers and 2 prior nonresponders. Notably, more than 80% of the patients who took at least 40% of the planned ribavirin dose achieved SVR. Most patients took ribavirin for the full 24 weeks, resulting in an SVR rate of 89.7% in these patients. A similar trend was observed for telaprevir, where ingestion of at least 60% of the total planned amount of the drug and a minimum of 8 weeks of administration was necessary to achieve an 80% SVR rate. For peg-interferon, at least 80% of the planned amount of the drug and continuation over the full 24 weeks of therapy was necessary to achieve an 80% SVR rate.

Multivariate analysis of factors associated with SVR

We assessed factors associated with SVR by logistic regression analysis. In univariate analysis, the following factors were significantly associated with SVR, telaprevir, ribavirin and peg-interferon adherence; age, baseline platelet, haemoglobin, AST, γGPT levels, total cholesterol and HDL; and the genotype of the IFNλ4 locus and core70 substitutions (Table 2). In a multivariate analysis of these factors, only baseline platelet levels, genotype of the IFNλ4 locus and peg-interferon were independent predictors for SVR.

Treatment discontinuation due to adverse events

The treatment was discontinued in 60 of the 273 patients (22.0%) due to anaemia (35%), nonvirological response